A critical review on heat transfer of supercritical fluids

WANG, Qingyang, XU, Jinliang, ZHANG, Chengrui, HAO, Bingtao and CHENG, Lixin

A critical review on heat transfer of supercritical fluids

Qingyang Wang[a,b], Jinliang Xu[a,b,*], Chengrui Zhang[a], Bingtao Hao[a] and Lixin Cheng[c]

[a] Beijing Key Laboratory of Multiphase Flow and Heat Transfer for Low Grade Energy Utilization, North China Electric Power University, Beijing, 102206, China

[b] Key Laboratory of Power Station Energy Transfer Conversion and System, North China Electric Power University, Ministry of Education, Beijing, 102206, China

[c] Department of Engineering and Mathematics, Sheffield Hallam University, City Campus, Howard Street, Sheffield S1 1WB, UK

ABSTRACT

Supercritical fluids have been widely used in a variety of applications, in which heat transfer under supercritical pressure is of great importance. This paper presents a critical review on supercritical heat transfer. Instead of giving an exhaustive review for the abundant existing literature, this paper provides a brief summary on the past work focusing on in-tube heat transfer and the pseudo-boiling concept, discusses the understanding of the mechanisms of supercritical heat transfer, and proposes suggestions for future work. For supercritical fluids heated in tubes, the typical characteristics observed in the experiments and the effects of different parameters and working conditions including mass flux, heat flux, pressure, tube diameter and flow direction are

discussed; the existing discoveries on the buoyancy and flow acceleration effects and the heat transfer deterioration phenomenon are discussed; and the heat transfer correlations and numerical methodologies are briefly summarized. For supercritical fluids cooled in tubes, the experimental observations and explanations, the proposed heat transfer correlations, and the numerical results are summarized and discussed. More importantly, this review provides a comprehensive review of the supercritical pseudo-boiling concept, which has received great attention in recent years. The experimentally observed pseudo-boiling phenomenon is first reviewed, and the theoretical studies for supercritical fluids to reveal their heterogenous two-phase features are summarized. The progress in the application of the pseudo-boiling concept on supercritical heat transfer is also discussed. Finally, suggestions for future research are provided to further advance the understanding and enable accurate prediction of supercritical heat transfer, recommending efforts to expand the experimental database for supercritical heat transfer, to utilize the experimental and numerical methodologies of subcritical two-phase flow in supercritical conditions, and to explore the supercritical surface tension concept for constructing a complete supercritical multiphase framework.

*Address correspondence to Prof. Jinliang Xu, Beijing Key Laboratory of Multiphase Flow and Heat Transfer for Low Grade Energy Utilization, North China Electric Power University, Beijing, 102206, P. R. China. E-mail: xjl@ncepu.edu.cn

Introduction

Since their first discovery in 1822 by Baron Charles Cagniard de la Tour, supercritical fluids (SFs) have attracted intensive research interests and have been widely used in a variety of applications, due to their unique and favorable properties and characteristics [1]. These applications include chemical and biochemical reactions [2], gasification [3], materials synthesis [4], separation and extraction of solids and liquids [5], waste water treatment [6], and many more. Heat transfer of SFs plays an important role in many of these applications. For example, in thermal-power engineering, supercritical water or CO_2 operate in cycles to convert thermal energy into power, where the SFs absorb or release heat in the heaters, heat exchangers (recuperators), and coolers [7-10], as shown in Fig. 1a (replotted from Ref. [7]). In transcritical CO_2 refrigeration cycles, the supercritical CO_2 is cooled in the gas coolers to complete the cycle [11, 12], as shown in Fig. 1b [12].

The 26th Conference of the Parties (COP26) of the United Nations Framework Convention on Climate Change was held in November 2021, marking an important milestone for the global response to climate change. China announced the commitments of peaking carbon dioxide emission before 2030 and achieving carbon neutrality before 2060. The European Union and the United Kingdom aim to be climate-neutral by 2050 with net zero greenhouse gas emissions. The United States also announced the target to reduce greenhouse gas pollution by 50~52% from 2005 levels in 2030. Reducing and eventually eliminating net CO_2 emission and achieving a net-zero world is a collaborate goal for the entire planet.

The two cycles shown in Fig. 1 can help to reduce greenhouse gas emission. Supercritical CO_2 Brayton cycles can use various energy sources including fossil fuel, solar energy, geothermal heat, nuclear energy, and waste heat, and have great benefit due to its flexibility and higher efficiency [7, 13]. Therefore, supercritical CO_2 power generation is attracting significant interests as a possible solution to carbon emission reduction. Moreover, the traditional refrigeration cycles use chlorofluorocarbons and hydrochlorofluorocarbons as refrigerants, which causes significant global warming and ozone depletion. CO_2 (R744) is a natural refrigerant, which is non-toxic, non-flammable and easy to obtain, and has an ozone depletion potential of 0 and a global warming potential of 1. Hence, transcritical CO_2 refrigeration cycles are much more environmentally-friendly compared to traditional refrigeration cycles.

Due to the important application of SFs in power generation and refrigeration cycles, understanding the mechanisms and obtaining the characteristics of supercritical heat transfer (SHT) is of significant importance to the design and operation of these systems. For example, the printed circuit heat exchanger (PCHE) is considered a promising candidate for heat transfer components in supercritical CO_2 cycles [14]. Straight channels [15, 16], zigzag channels [17-20], S-shape channels [21], and airfoil fin channels [22-24] have been used for PCHE. Moreover, micro-tube bundles have been used as the gas cooler structure for the application of CO_2 refrigeration cycles [25-27], and the cooling heat transfer characteristics of supercritical CO_2 in this structure governs the cycle performance. Therefore, there have been extensive research interests in SHT with numerous papers published in the literature. Efforts made in the past several decades have

significantly advanced the understanding of SHT and the ability to accurately predict SHT. In this paper, we aim to provide a critical review on the heat transfer of SFs. The objective is not to provide an exhaustive list of previous publications about SHT, but to highlight the recent progress made by researchers on understanding SHT, and more importantly, to give perspectives on future work and point out potential pathways to further reveal the underlying mechanisms of SHT. We try not to repeat the efforts of existing review articles, but to focus our attention on the pseudo-boiling concept. The present paper is structured as follows: we first provide a brief introduction of SFs and SHT, followed by discussion of the unique properties of SFs that governs SHT. Then, we provide a literature review on SHT in tubes, including both heating and cooling heat transfer. We then discuss the concept of pseudo-boiling in SHT, which is attracting increasing interests over the past decade. Finally, we provide our perspectives on SHT and discuss possible future research directions.

Thermophysical properties of SFs

Although SFs are considered single phase fluid according to classical thermodynamic theory, it has long been recognized that heat transfer under supercritical pressures is significantly different compared with that of single-phase convection of constant property fluid, due to the extreme variation of thermophysical properties of SFs. Fig. 2 shows the variation of thermophysical properties of two most widely used SFs, with Fig. 2a showing water at 24 MPa and Fig. 2b showing CO_2 at 9 MPa (the pressures are chosen arbitrarily).

Under a constant supercritical pressure, the specific heat capacity attains a peak value at the pseudo-critical temperature T_{pc}, and the density, thermal conductivity, and viscosity vary substantially with temperature near T_{pc}, showing sharp decrease when crossing T_{pc} from low temperature to high temperature. T_{pc} increases with increasing supercritical pressure, and the pseudo-critical points under different pressures form a special line in the *P*-*T* phase diagram, called the Widom line, which will be discussed in more details later. With increasing pressure, the variations become less significant, and the specific heat also displays wider and shorter peak shape.

The sharp variations of thermophysical properties near T_{pc} result in two unique heat transfer phenomena widely observed in SHT: heat transfer enhancement (HTE) and heat transfer deterioration (HTD). On the one hand, the significant increase of specific heat capacity near T_{pc} allows the fluid to absorb (or release) more heat under given mass flow rate, which renders HTE; on the other hand, the drastic decrease of fluid thermal conductivity with increasing temperature causes less efficient heat transfer and consequently HTD. Due to the combined effect of enhancement and deterioration, three modes of heat transfer exist in supercritical conditions, namely, normal heat transfer (NHT), HTE, and HTD. Extensive efforts have been made in the past to study and understand SHT.

Supercritical fluids heated in tubes

Experimental investigations

Due to the development of the idea of using supercritical water to increase the thermal

efficiency of power plants, heat transfer of supercritical water has been extensively investigated in the past century. In recent years, heat transfer of supercritical CO_2 (SCO_2) has also gained substantial interests due to the need to develop SCO_2 cycles for power generation, which can utilize various heat sources, and potentially achieve higher efficiency and more flexibility. There have been several comprehensive review papers focusing on the in-tube heat transfer of supercritical water [28, 29] and CO_2 [30-32]. Tables 1 and 2 present lists of recent experimental studies on SF heated in circular tubes, with Table 1 listing Refs. [33-43] for supercritical CO_2 and Table 2 listing Refs. [44-52] for supercritical water. As mentioned above, three heat transfer modes are usually observed: NHT, HTE, and HTD. With various working conditions and flow directions, the heat transfer characteristics are different. Generally, SCO_2 attains smaller heat transfer coefficient (HTC) than supercritical water under similar conditions, due to their different thermophysical properties.

Typical heat transfer characteristics. For SHT in tubes, the wall temperature variation and HTC variation along the tube are commonly plotted against the bulk fluid enthalpy. The NHT and HTE modes are sometimes hard to differentiate from each other and are thus grouped together to be considered as NHT. Fig. 3a shows a typical NHT case reported in Ref. [40], for CO_2 at 20.822 MPa heated in a tube with inner diameter of 10 mm. The inner wall heat flux and mass flux are 355.45 kW/m^2 and 1001.5 kg/m^{2}s, respectively. As the SF is heated along the tube, the bulk fluid temperature increases gradually, and wall temperature also increases. The HTC first increases and then decreases with increasing bulk fluid enthalpy, reaching a peak value near (usually before) the pseudo-critical point. Fig. 3b shows a typical HTD case for CO_2 at 8.221 MPa, with inner wall

heat flux of 244.33 kW/m^2 and mass flux of 744.5 kg/m^{2}s, reported also in Ref. [40]. Different from the monotonic increase of wall temperature along the tube, the wall temperature profile for HTD case shows one or multiple obvious peak(s) before the bulk fluid temperature reaches pseudo-critical temperature. The wall temperature peak results in a valley at the corresponding location on the HTC curve. Both cases shown in Fig. 3 are based on vertical tubes with uniform heating, while for inclined and horizontal tubes, heat transfer in the circumferential direction is no longer uniform. Due to the sharp variation of density of SF, lighter (gas-like) fluid with lower thermal conductivity will accumulate on the top of the tube while heavier (liquid-like) fluid with higher thermal conductivity will accumulate at the bottom. Therefore, for inclined and horizontal tubes, the wall temperature at the top generatrix is higher than that at the bottom generatrix, and consequently, the HTC at the top generatrix is smaller than that at the bottom generatrix. Fig. 4 shows the experimental curves for supercritical water at 25 MPa heated in a horizontal tube [47], clearly showing the difference between top and bottom of the tube. It is worth noting that due to the non-uniform distributions of both flow field and temperature field in each cross-section, the heat flux is also non-uniform in the circumferential direction. Experimentally, in-tube heat transfer is usually investigated by measuring the outer tube wall temperature and extracting the inner wall temperature to calculate HTC. For inclined and horizontal tubes, the inner wall temperature and heat flux cannot be trivially calculated assuming uniform heat flux distribution. Therefore, the solution from an inverse heat conduction problem should be used [53].

Effect of mass flux. For both supercritical water and CO_2, the heat transfer behaviors vary

with different mass flux. Generally, the HTC increases with increasing mass flux, due to the increasing turbulence. With low mass flux, HTD tends to occur, and the HTD behavior disappears with increased mass flux [54]. Ackerman [55] conducted experiments for supercritical water heat transfer in a vertical smooth tube with an inner diameter of 9.4 mm and a length of 1.83 m at pressure of 31 MPa. With a constant heat flux of 473.2 kW/m^2 and the mass flux covering three values of 542.5, 678.1 and 1220.6 kg/m^2s, it is found that with increasing mass flux, the wall temperature decreases, indicating increased HTC. The HTD phenomenon, characterized by wall temperature peaking feature, occurs only at the smallest mass flux value, and disappears at the two larger mass fluxes. For SCO_2, Shiralkar and Griffith [56] observed similar trend: for SCO_2 flowing upward at 7.58 MPa in a vertical tube with inner diameter of 6.35 mm, the wall temperature decreased with increasing mass flux, and HTD was observed for low mass flux conditions. However, different trend has also been reported [57, 58], showing decreased HTC with increasing mass flux under certain conditions. In a comprehensive review article [59], this observed anomaly was discussed, and the reason was attributed to the counteracting effects of Reynolds number and property variation at low heat flux ranges.

Effect of heat flux. It has been widely reported that HTD usually occurs with large heat flux, accompanied by significant wall temperature peaks. However, the effect of heat flux on HTC is complex and different trends have been observed, which is likely due to the competing effects of HTE and HTD as discussed before. Far away from the pseudo-critical point, heat flux usually has insignificant effect on the HTC due to the small variation of thermophysical properties [47]. For

NHT and HTE cases at low heat flux, there is an HTC peak at the vicinity of the pseudo-critical point, which gradually diminishes with increasing heat flux [40, 49]. Further increase of heat flux will results in the transition into HTD regime, where wall temperature peak appears. With increasing heat flux, the position of the peak moves towards the inlet and the magnitude of the peak increases [44, 51, 55].

Effect of pressure. Because the variation of thermophysical properties of SFs becomes less severe with increasing pressure, both the effect causing HTE and that causing HTD are suppressed at higher pressures. Hence, it is usually observed that at high supercritical pressures, the HTC peak for NHT regime and the wall temperature peak for HTD regime are usually wide and short or even do not appear at all [40]. In other words, for NHT regime, when the pressure is closer to the critical pressure, the HTC peak is more significant [60, 61]; for HTD regime, larger pressure helps to suppress the HTD [62]. Moreover, due to the increased pseudo-critical temperature with increasing pressure, the HTC peak or wall temperature peak will also shift towards larger bulk fluid temperature and enthalpy [63]. Generally, the heat transfer characteristics at very high supercritical pressure will become very similar to those of single-phase convection.

Effect of tube diameter. Yildiz [64] provided a comprehensive review on the effect of tube diameter on SHT. Due to the complex effects causing both HTE and HTD, the effect of tube diameter is also complicated. In NHT regime, the HTC usually increases with decreasing tube diameter [65], which can be understood by looking at the convective heat transfer correlations. With the same working conditions, the correlations usually predict the same Nusselt number, and

larger tube diameter results in smaller HTC according to the definition of Nusselt number. It is also found that HTD is more likely to occur with large tube diameter while HTD is suppressed with small tube diameter [65-67], due to the buoyancy force caused by the variation of fluid density. Zhang et al. [43] found that the tube diameter has no obvious effect on the transition boundary between NHT and HTD, but affects the magnitude of the temperature peak during HTD. In HTD regime, larger tube diameter usually results in smaller HTC, although different trends have been reported. For examples, Yamashita et al. [68] noted no effect from tube diameter on SHT in the HTD regime, while Bae et al. [66] found that with larger tube diameter, the HTC is higher than that for smaller diameter when the bulk fluid enthalpy is below certain value.

Effect of flow direction. For vertical tubes, the difference of heat transfer characteristics between upward and downward flows has been widely observed, which are attributed to the buoyancy effect. Bourke et al. [69] found that at low heat fluxes, there is nearly no difference between upward flow and downward flow; with increasing heat flux, HTD occurs for upward flow while NHT is remained for downward flow. Similar trend was also observed in Refs. [70, 71]. However, Liao and Zhao [72] studied SCO_2 heated in miniature tubes (with inner diameters ranging from 0.5 to 2.16 mm) and observed that HTD occurs for downward flow while HTE occurred for upward and horizontal flows, which is inconsistent with the trend reported for large diameter tubes. Jiang et al. [73] found that for small tube diameter of 0.27 mm at low Reynolds number and high heat flux, both upward and downward flows showed HTD behavior. For horizontal tubes and inclined upward tubes, non-uniform temperature distribution exists in the

circumferential direction. Due to the accumulation of low-density fluid near the top of the tube, the wall temperature at the top generatrix is larger than that at the bottom generatrix, and correspondingly, the HTC at the top is smaller than at the bottom [47, 74, 75]. The difference is more significant for larger tube diameter, higher heat flux, and smaller mass flux.

Buoyancy and flow acceleration effects

In most previous experimental studies, the observed abnormal behaviors of SHT including HTE and HTD are attributed to the buoyancy effect and flow acceleration effect resulted from sharp variation of the thermophysical properties of SFs. Table 3 and Table 4 show the buoyancy parameters [37, 76-85] and flow acceleration parameters [35, 37, 79, 81, 82, 86, 87] reported in the literature, respectively.

When SFs flows inside a heated tube, the fluid near the wall has a higher temperature than the bulk fluid in the tube core, which causes a temperature gradient near the wall at the tube cross-section. Due to the drastic variation of properties of SFs near the pseudo-critical temperature, the temperature gradient results in the existence of density gradient, and consequently, buoyancy force. The buoyancy force changes the velocity distribution of the fluid, which then results in the variation of shear force within the fluid, and finally affect heat transfer of the fluid. Different researchers proposed different dimensionless numbers to quantify the influence of buoyancy force on SHT. Jackson et al. [77] proposed the following dimensionless parameter, which is widely used now to determine whether buoyancy affects heat transfer:

$$Bu = \frac{Gr_{\mathrm{b}}}{Re_{\mathrm{b}}^{2.7}} \tag{1a}$$

where

$$Re_{\mathrm{b}} = \frac{Gd_{\mathrm{in}}}{\mu_{\mathrm{b}}} \tag{1b}$$

$$Gr_{\mathrm{b}} = \frac{g\rho_{\mathrm{b}}(\rho_{\mathrm{b}}-\rho_{\mathrm{ave}})d_{\mathrm{in}}^3}{\mu_{\mathrm{b}}^2} \tag{1c}$$

$$\rho_{\mathrm{ave}} = \frac{\int_{T_{\mathrm{b}}}^{T_{\mathrm{w}}} \rho dT}{T_{\mathrm{w}}-T_{\mathrm{b}}} \tag{1d}$$

The subscripts b, ave, and w represent bulk fluid, average, and wall conditions, respectively. When $Bu<10^{-5}$, the effect of buoyancy force is considered to be negligible.

Jackson et al. [80] derived a new dimensionless parameter Bu^* to characterize the effect of buoyancy force to SHT:

$$Bu^* = \frac{Gr^*}{Re_{\mathrm{b}}^{3.425}Pr_{\mathrm{b}}^{0.8}} \tag{2a}$$

where

$$Re_{\mathrm{b}} = \frac{Gd_{\mathrm{in}}}{\mu_{\mathrm{b}}} \tag{2b}$$

$$Pr_{\mathrm{b}} = \frac{\mu c_{\mathrm{p}}}{\lambda} \tag{2c}$$

$$Gr^* = \frac{g\beta_{\mathrm{b}}q_{\mathrm{w}}d_{\mathrm{in}}^4}{\lambda_{\mathrm{b}}\nu_{\mathrm{b}}^2} \tag{2d}$$

Here, β is the volumetric expansivity. It is assumed that when $Bu^*<6\times10^{-7}$, the buoyancy effect can be neglected; when $6\times10^{-7}<Bu^*<8\times10^{-6}$, the buoyancy effect causes deteriorated heat transfer in the tube; and when $Bu^*>8\times10^{-6}$, the buoyancy effect enhances heat transfer.

The different parameters to describe buoyancy effect are derived from the governing equations under certain assumptions, and the threshold values determining whether buoyancy effect is

significant or not are obtained based on experimental results. When different buoyancy parameters are calculated and compared with experiments, they could produce different conclusions, sometimes contradictory to each other. Huang et al. [88] provided a comprehensive review for the buoyancy effect in SHT. By comparing the different buoyancy criteria proposed in the literature, it is found that for different experiments, even using the same buoyancy parameter, the obtained threshold values are different. Currently, there is no general criterion suitable for different SFs and working conditions. Moreover, the buoyancy effect is dependent on the flow direction: for horizontal flows, the buoyancy effect results in higher wall temperature and lower HTC at the top generatrix of the tube; for vertical flows, the buoyancy effect deteriorates heat transfer for upward flow and enhances heat transfer for downward flow.

Besides the buoyancy effect, the flow acceleration also affects SHT. McEligot and Jackson [89] found that when SF flows in a heated tube, the bulk fluid temperature increases and consequently the bulk fluid density decreases along the tube, causing increased fluid velocity. The flow laminarization occurs and results in deteriorated heat transfer. A widely used dimensionless parameter to characterize the flow acceleration effect is proposed by McEligot [87] as

$$K_{\mathrm{v}} = \frac{4q_{\mathrm{w}}d_{\mathrm{in}}\beta_{\mathrm{b}}}{Re_{\mathrm{b}}^{2}\mu_{\mathrm{b}}c_{\mathrm{p}}} \tag{3}$$

McEligot [87] concluded that when $K_{\mathrm{v}}>3\times10^{-6}$, the flow acceleration effect is significant and can cause HTD; while when $K_{\mathrm{v}}<3\times10^{-6}$, the flow acceleration effect can be negligible. Different researchers proposed different threshold values of K_{v} based on their own experiments.

Jiang et al. [35] investigated heat transfer of CO_2 in a vertical micro tube with inner diameter

of 99.2 μm under supercritical pressures, and found that both heating and pressure drop along the tube can cause flow acceleration in micro tubes. The following dimensionless number was proposed to incorporate the flow acceleration effect from both temperature increase and pressure drop:

$$K_{\mathrm{v}} = K_{\mathrm{v,T}} + K_{\mathrm{v,P}} = \frac{4q_{\mathrm{w}}d_{\mathrm{in}}\beta_{\mathrm{b}}}{Re_{\mathrm{b}}^{2}\mu_{\mathrm{b}}c_{\mathrm{p}}} + \frac{-d_{\mathrm{in}}}{Re_{\mathrm{b}}}\alpha_{\mathrm{T}}\frac{dT}{dx} \tag{4}$$

where $K_{\mathrm{v,T}}$ and $K_{\mathrm{v,P}}$ represent the flow acceleration due to heating and pressure drop, respectively, β and α_{T} are the volumetric expansivity and isothermal compressibility, respectively. Zhao et al. [90] compared the buoyancy and flow acceleration effects in vertical tubes with inner diameters of 0.27 mm and 2.0 mm, and found that the flow acceleration effect dominates in the small diameter tube, while the buoyancy effect dominates in the larger diameter tube. The flow acceleration effect is not affected by the flow direction, since flow acceleration always occurs along the flow direction.

Heat transfer deterioration

As discussed before, HTD is a unique phenomenon observed in SHT, which causes significant wall temperature rise, resulting in safety issues due to overheating of the components. One important issue about HTD is the identification of HTD from experiments, i.e., how to define HTD. Different methods have been reported in the literature. Zhang et al. [91] reviewed past literature and categorized them into three types of HTD definition. The first type is identified based on the wall temperature peaking phenomenon, meaning that if there is a wall temperature peak along the

tube, it is considered HTD, while if the wall temperature profile is monotonic, it is considered non-HTD. The second type is identified based on comparison of the experimental heat transfer performance to that predicted by single-phase correlation, usually the Dittus-Boelter (DB) correlation: when the ratio of the experimental *Nu* (or HTC) and the predicted *Nu* (or HTC) is below certain threshold value, it is considered HTD. It is noted that the threshold value is somewhat arbitrary, and both the bulk fluid state and a fixed reference state have been used to calculate the correlation value. The third type is identified based on a particular temperature limit dependent on the materials used: when the wall temperature exceeds this temperature limit, it is considered HTD. The HTD cases identified by these three methods can be very different, which results in difficulties in obtaining a universal definition of HTD [91]. In most published works, the first type of definition is utilized for vertical tubes, while the HTD definition for horizontal tubes is usually not mentioned in the papers. However, for vertical tubes, determining whether a wall temperature peak exists or not along the tube is not simple, because fluctuation of the wall temperature profile can exist due to the inevitable error of wall temperature measurement. In Ref. [40], an 8 °C threshold is used to define the peak to avoid uncertainty of temperature measurement using thermocouples.

Due to the importance of the accurate prediction of the transition from HTE to HTD for safety concern, numerous works have been conducted to address this need. Luo et al. [92] compared different HTD criteria proposed in the literature. Notably, Zhu et al. [40] proposed a supercritical boiling number (*SBO*) based on the supercritical pseudo-boiling concept, and developed a HTD criterion based on the *SBO* as

$$q_{\mathrm{CHF}} = SBO \times G \times i_{\mathrm{pc}} \quad (5)$$

where q_{CHF} is the transition heat flux, G and i_{pc} are the mass flux and pseudo-critical enthalpy of the fluid, respectively. This criterion demonstrates accuracy for four different working fluids including CO_2, H_2O, R134a, and R22, with different *SBO* values for different fluids [93]. The details of the pseudo-boiling concept will be discussed in the section for pseudo-boiling later.

Heat transfer correlations

Most previous experimental studies for supercritical heat transfer have found that the traditional convective heat transfer correlations for constant-property fluids do not agree well with experimental results due to the unique characteristics of SFs. Hence, many researchers developed and proposed heat transfer correlations based on their experimental results. Table 5 shows the selected correlations for supercritical CO_2 and water heated in tubes [34, 37, 45, 51, 61, 81, 94-98]. These correlations are mostly originated from the classical single-phase convection correlations, such as the DB correlation or the Gnielinski correlation, with additional correction terms. The correction terms can include the variation of density and specific heat of the fluid at wall temperature with respect to the bulk temperature, the buoyancy and/or flow acceleration effects, and working conditions or structural parameters such as heat flux, mass flux, tube diameter, etc. A semi-empirical correlation considering the buoyancy and flow acceleration effects under HTD conditions was also developed by Li and Bai [99]. Reviews of the heat transfer correlations have been provided in Ref. [28] for supercritical water and Ref. [100] for SCO_2.

Recently, different from the correlations based on single-phase framework, Zhu et al. [98] emphasized the multiphase flow structure for SFs to define a dimensionless supercritical K number, and proposed a correlation for SHT incorporating the supercritical K number. For forced convective heat transfer under heating condition at supercritical pressure, this correlation shows superior accuracy with smaller errors compared with the commonly used correlations from literature, and is suitable for both HTD and NHT regimes with wide parameter ranges. Details of this correlation will be discussed later.

Numerical modeling

Besides experimental investigations, there are also extensive numerical studies of SHT. The existing numerical modeling of SHT can be categorized into three types: direct numerical simulation (DNS), large eddy simulation (LES), and Reynolds-averaged Navier-Stokes (RANS). Many numerical studies are performed using commercial CFD software such as Ansys Fluent and CFX, for different tube configurations including bare tubes with vertical, horizontal and inclined orientation, and structured tubes such as spiral, grooved and dimpled tubes. Most of the working conditions encountered in engineering practice are turbulent flow conditions, and the accuracy of the numerical simulation mainly depends on the selected turbulence model. Different researchers have used different turbulence models to calculate, evaluate and analyze SHT.

Widely used turbulence models include the k-ε model (including standard k-ε, Re-normalization group (RNG) k-ε, and Realizable k-ε), the low Re turbulence models, and the k-ω

models (including standard k-ω and shear-stress transport (SST) k-ω). Seo et al. [84] performed numerical simulation for supercritical water in a vertical tube using the standard k-ε model, and found that the model agrees well with the experimental results from Yamagata et al. [101]. Zhang et al. [102] compared standard k-ε model, RNG k-ε model and Realizable k-ε model with Ref. [101]'s experimental results, and also concluded that the standard k-ε model has better prediction accuracy. Wang et al. [103] combined a turbulent Prandtl number model into a low *Re* turbulence model, and found the validity of the field synergy principle in supercritical conditions. The most commonly used model for supercritical heat transfer is the SST k-ω model [104-110], which has been shown to attain small error against experimental data. Palko and Anglart [104] studied HTD phenomenon in a vertical tube using the SST k-ω model, and compared the predicted wall temperature with the experimental results of Shitsman [111] and Ornatskij et al. [112]. The model captures the two-peak phenomenon observed in the experimental wall temperature profile and predicts the wall temperature peak position accurately. Wang et al. [113] compared the prediction accuracy of different models, and found that the SST k-ω model shows the best prediction accuracy with the maximum error between simulation and experiment approaching ~10%. Other researchers modified the turbulence model and compared with the existing models [114-118]. In particular, it is found that using the SST k-ω model with the variable turbulent Prandtl number model provides more accurate prediction, especially for HTD cases [119-121].

Ničeno et al. [122] studied heat transfer of supercritical water in vertical upward and downward tubes using LES, and found good agreement between simulation and experiments. The

model not only captures the trend of wall temperature variation, but also match with the wall temperature values quite well. To reduce the computational cost, the grid was divided for flow between two parallel walls with the hydraulic diameter equal to the circular tube. The sub-grid scale model was chosen as the WALE model [123], since it damps the near-wall eddy viscosity while also stabilizes the calculation. Bae et al. [124] used DNS to simulate the heat transfer of SCO_2 in vertical upward and downward tubes, and found HTD in upward flow while no HTD in downward flow. Chu et al. [125] simulated SCO_2 flow in horizontal tubes, and found that flow stratification occurs in the tube. For now, DNS can only be used to calculate simple cases of SHT and cannot be used for large scale engineering simulation.

Supercritical fluids cooled in tubes

Compared to heating of SFs in tubes, cooling heat transfer of SFs in tubes has attracted less attention, and only a few dozen papers exist in the literature. They are mostly published in the 21st century, which is enabled by attention on the trans-critical CO_2 refrigeration cycle due to the more environmentally friendly properties of CO_2 compared with traditional refrigerants.

Experimental investigations. A number of studies have been reported for cooling heat transfer of SCO_2 in tubes. Most cooling experiments are conducted using a tube-in-tube heat exchanger configuration, flowing SCO_2 inside the inner tube and coolant fluid inside the annulus. Table 3 lists the recent experimental studies for supercritical CO_2 cooled in tubes from Refs. [126-135]. A commonly observed phenomenon is that as the bulk fluid temperature decreases along the

tube and passes the pseudo-critical temperature, the HTC first increases and then decreases, presenting a peak value. The peak value usually occurs when the bulk fluid temperature is close to and slightly higher than the pseudo-critical temperature. This is because the specific heat capacity of the fluid reaches maximum near the pseudo-critical point, and during the cooling process, the bulk fluid temperature is higher than the near wall fluid temperature. Fig. 5 shows the experimental results from Ref. [130] for CO_2 cooled in a horizontal tube, showing the appearance of an HTC peak for various operating pressures. It is worth noting that in-tube heat transfer with heating and cooling conditions have quite different characteristics. One major difference is that HTD could occur for heating conditions, while for cooling conditions there is always enhanced heat transfer near the pseudocritical point.

The effects of mass flux, pressure, and tube diameter are analyzed by researchers. Many studies reported similar observations. With increasing mass flux, the local HTC increases, due to the increased turbulent diffusion. As the operating pressure increases, the peak value of HTC decreases, which is due to the decreased peak specific heat value with increasing pressure [26, 135-137]. Dang and Hihara [126] found that the HTC values are not affected by the pressure when the bulk fluid temperature is far away from the pseudo-critical temperature. Similar conclusions are also drawn in Refs. [127, 129]. Zhang et al. [132] showed that the HTC decreases with increasing pressure at low bulk fluid temperatures but increases with pressure at high bulk fluid temperatures. Regarding the effect of tube diameter, it was usually found that the HTC decreases with increasing tube diameter, which is consistent with common convective heat transfer behavior

[126, 132, 136]. However, it is worth noting that different studies presented their results in different forms, such as *Nu* or HTC times tube diameter, which may cause confusion when comparing results among different papers. Zhang et al. [132] also showed that for horizontal tubes, with increasing tube inner diameter, the peak value of HTC decreases. This is attributed to the buoyancy effect, which causes non-uniform wall temperature distribution and worse heat transfer. However, the effect of heat flux on cooling heat transfer is rarely discussed in the literature, which is probably because it is difficult to accurately control the cooling heat flux experimentally. Moreover, we have not found existing literature discussing the effect of flow direction during cooling heat transfer.

Heat transfer correlations. There have been plenty of correlations proposed in the literature for supercritical cooling heat transfer. Table 7 shows the selected correlations for cooling of SCO2 reported in the literature [126, 127, 130, 132, 135-139]. In general, similar to the case of heating conditions, the existing correlations for supercritical cooling heat transfer are also mostly based on single-phase convective correlations with additional correction terms. Fang et al. [140], Cheng et al.[141], Lin et al. [142] and Ehsan et al. [30] provided review and comparison of different heat transfer correlations for supercritical cooling proposed in the literature. It is observed that many existing correlations are only suitable for some particular data ranges or experimental configurations, and cannot be applicable for wide ranges of operating parameters and tube diameters.

Numerical investigations. Numerical studies on cooling heat transfer of SCO_2 have been reported in the literature [132, 143-154], investigating the effects of multiple parameters on the

cooling heat transfer performance, including tube diameter, mass flux, heat flux, pressure, and inlet temperature. Most of these works show qualitative agreement with the experimental observations, especially the appearance of an HTC peak along the tube at the location where the bulk fluid temperature is close and slightly larger than the pseudo-critical temperature. However, the quantitative results obtained from numerical simulations display significant difference compared with the results calculated from correlations. It is worth noting that in many numerical studies [149-153], it was observed that for SCO_2 cooled in horizontal and inclined tubes, stratification-like phenomenon and secondary flows occur in the tube cross-section. When the bulk fluid temperature is higher than the pseudo-critical temperature, the fluid near the top of the tube cross-section is lighter with smaller density and the fluid near the bottom of the cross-section is heavier with larger density. The stratification results in secondary flow and consequently radial disturbance. HTC at the top generatrix is also higher than that at the bottom generatrix. This stratification phenomenon is attributed to the buoyancy effect caused by the sharp variation of thermophysical properties near the pseudo-critical point.

Supercritical pseudo-boiling

In classical thermodynamic theory, SF is regarded as homogeneous, continuous and single-phase. Different from constant-property fluid, SF has significant variation of thermophysical properties near the pseudo-critical point. Hence, in most previous studies for SHT, the single-phase assumption for SFs is applied, and the sharp variation of properties is taken into consideration, as

discussed in previous sections.

The supercritical pseudo-boiling phenomenon has been observed decades ago. In 1956, Goldmann [155] observed an abnormal and striking behavior for supercritical water heated in a tube: under certain high heat flux, the tube produced a loud whistling noise very similar to that produced during subcritical boiling experiments. Ackerman [55] found that film-boiling-like SCPB occurs in smooth tubes while it can be suppressed by using ribbed internal tube surface, similar to the suppression of subcritical film boiling using structured surfaces. Holmann et al. [156] observed boiling-like phenomenon with vapor trails in the photos of the experiments for R12 heat transfer at the critical pressure. Stewart et al. [157] observed pressure oscillation of supercritical water flowing in a heated horizontal tube. Similar behavior was also observed by Kafengauz and Fedorov [158] in their experiments using supercritical diisopropylcyclohexane, and was attributed to the pseudo-boiling phenomenon. Kafengauz and Fedorov [159] concluded that supercritical pseudo-boiling occurs when $T_w > T_{pc} > T_b$, where T_w, T_{pc}, and T_b represent wall, pseudo-critical, and bulk fluid temperatures, respectively. This temperature range can be very large since T_w can be much higher than T_b. Sakurai et al. [160] conducted visualization study of SCO_2 heat transfer and obtained density gradient distribution from shadowgraphs, which provides evidence to the pseudo-boiling phenomenon. Ambrosini [161] found that density-wave and Ledinegg instabilities exist in SCFs in heated channels, which are the same characteristics observed in subcritical boiling channels. Tamba et al. [162] conducted pool boiling experiments with CO_2 at both subcritical and supercritical pressures, and observed similar behaviors: with the increase of heat flux at

supercritical pressure, bubble-like, vapor-column-like, and vapor-film-like features appear consecutively, corresponding to the transition from nucleate to film boiling at subcritical pressure.

As mentioned before, in traditional thermodynamic theory, SF is considered a homogeneous single-phase fluid. Nevertheless, under a given supercritical pressure, SF demonstrates vastly different properties when crossing the pseudo-critical temperature T_{pc}, as shown in Fig. 2. The specific heat capacity c_p reaches a peak value at T_{pc}. The density, viscosity, and thermal conductivity decreases significantly when crossing T_{pc}, which is similar to the crossing of liquid-vapor equilibrium line at subcritical pressures. This inspires researchers to divide SF into liquid-like (LL) and gas-like (GL) phases by T_{pc}.

The Widom line (WL) is the connection of the pseudo-critical points in the P-T phase diagram. By inelastic X-ray scattering and molecular dynamics (MD) simulations, Simeoni et al. [163] found that although first-order phase transition is absent in supercritical conditions, the WL can still divide the supercritical region into LL and GL regions due to their different dynamic behavior. Gallo et al. [164] used MD simulations to reveal that the transport properties of supercritical water transition sharply from LL to GL when crossing the WL. Banuti [165] developed pseudo-boiling transition temperatures for SFs to cross the WL, in which the WL divides the supercritical domain into a GL region and a LL region. Ha et al. [166] introduced machine learning method in MD simulations to label molecules as either LL or GL, and identified a “Widom delta” consisting of LL and GL molecules in microscopic view. Maxim et al. [167] applied neutron imaging techniques and visualized rapid conversion of density from LL to GL in supercritical water when crossing the

WL. Further, Maxim et al. [168] combined the neutron imaging technique with MD simulations and demonstrated the phase transition of supercritical water across the WL. Recently, Xu et al. [169] proposed the three-regime-model, adding a two-phase-like (TPL) regime besides the LL regime and the GL regime, as shown in Fig. 6. In the TPL regime, nanovoids were observed which have similar characteristics as the bubble characteristics in subcritical pressure. Hence, voids in the supercritical state were called “bubblelike” in Ref. [169]. Nonlinear analysis was also performed to demonstrate the chaotic behavior in the TPL regime, similar to subcritical two-phase flow.

In subcritical boiling, when liquid evaporates into vapor at the liquid-vapor interface of a bubble, the density difference between the two phases results in a larger velocity for the vapor phase. This will induce a force acting by the bubble to the surrounding liquid due to momentum change, and consequently the bubble is subject to a reaction force from the liquid, which is called the evaporation momentum force [170]. The evaporation momentum force is widely acknowledged to play an important role in subcritical boiling heat transfer [171]. Kandlikar [170] proposed two dimensionless numbers to describe the competition between the evaporation momentum force and the inertia force during flow boiling: the boiling number *Bo* and the *K* number. A large *Bo* (or *K*) indicates the dominance of evaporation momentum force, which tends to pin the bubbles on the wall and results in CHF; while a small *Bo* (or *K*) indicates the dominance of inertia force, which tends to detach the bubble from the wall.

For SHT, there is also competition between evaporation momentum and inertia forces during

LL to GL phase transition. Hence, the two dimensionless numbers discussed above were defined similarly to describe this competition. Zhu et al. [40] defined the supercritical boiling number (*SBO*) as

$$SBO = \frac{q}{G i_{\mathrm{pc}}} \tag{6}$$

where q, G, i_{pc} are the heat flux, mass flux, and pseudo-critical enthalpy, respectively. Based on experimental results of SCO_2 flowing upward inside a uniformly heated vertical tube, as well as the experimental results reported in the literature, Zhu et al. [40] found that a critical *SBO* of 5.126×10^{-4} can be used as the criterion for the transition between normal heat transfer (NHT) mode and heat transfer deterioration (HTD) mode: when $SBO<SBO_{\mathrm{cr}}$, NHT occurs; when $SBO>SBO_{\mathrm{cr}}$, HTD occurs. The results are presented in Fig. 7a, clearly showing the sharp transition when crossing the critical *SBO* value. The reason is that based on its physical meaning, when *SBO* is large, the evaporation momentum force dominates, resulting in the formation of GL film near the wall and consequently HTD; on the contrary, with small *SBO*, the inertia force dominates and tends to break the "vapor film".

The conclusion of using *SBO* as the transition criterion is further extended to other supercritical fluids including water, R134a, and R22 by Xu et al. [93], except with different SBO_{cr} values of 2.018×10^{-4}, 1.653×10^{-4} and 1.358×10^{-4}, respectively. Furthermore, Zhu et al. [172] conducted experiments of SCO_2 flowing upward in non-uniformly heated vertical tubes, and found that the transition from NHT to HTD can still be well-captured by a critical *SBO* of 8.908×10^{-4}, indicating that HTD is delayed by using non-uniform heating condition.

By analogy to subcritical *K* number, Zhu et al. [98] defined the supercritical *K* number as

$$K = (\frac{q}{Gi_{\mathrm{w}}})^2 \frac{\rho_{\mathrm{b}}}{\rho_{\mathrm{w}}} \tag{7}$$

where subscripts b and w represent bulk and wall conditions, respectively. Using 5560 data points for supercritical water, CO_2 and R134a heated in vertical tubes, Zhu et al. [98] proposed the following correlation for the HTC:

$$Nu = 0.0012 Re_{\mathrm{b}}^{0.9484} Pr_{\mathrm{b,ave}}^{0.718} K^{-0.0313} \tag{8}$$

where $Pr_{\mathrm{b,ave}}$ is the average bulk Prandtl number calculated by

$$Pr_{\mathrm{b,ave}} = \frac{\mu_{\mathrm{b}}}{\lambda_{\mathrm{b}}} \frac{i_{\mathrm{w}} - i_{\mathrm{b}}}{T_{\mathrm{w}} - T_{\mathrm{b}}} \tag{9}$$

To predict heat transfer characteristics using this correlation, iteration is needed to obtain the unknown wall temperature T_{w}. The prediction using this correlation shows the smallest error among the correlations for SHT, and can be widely applicable to different supercritical fluids, tube diameters, and working conditions. The negative exponent for *K* in the correlation means a larger *K* number suppresses heat transfer, which agrees with the physical meaning of *K*.

The vapor film formation near the tube wall not only affects heat transfer, but also affects fluid flow, which is termed as the "orifice contraction effect" by Zhang et al. [173]: they found that the friction factor *f* for HTD regime is much larger than that for NHT regime, due to the vapor film expansion forming an orifice to contract the flow. Based on pressure drop data for experiments using SCO_2, they included the *K* number to propose a correlation for the friction factor *f* as

$$f = 2.15 Re^{-0.342} K^{0.027} \tag{10}$$

which demonstrates small error over wide parameter ranges. Moreover, Zhang et al. [43] experimentally studied the HTD behavior with multiple wall temperature peaks, and found that

the friction factor is larger for multi-peak cases compared with the HTD cases with single temperature peak, which can be attributed to the formation of multiple GL orifices inducing multiple contraction on the flow, as shown in Fig. 7b.

Recently, Wang et al. [174] developed a three-regime-model, which is a comprehensive multiphase framework for SHT. The three regimes are the liquid-like (LL), vapor-like (VL, same as GL) and two-phase-like (TPL) regimes. The pseudo-vapor mass quality x for SFs is newly defined, and $x<0$, $0<x<1$ and $x>1$ correspond to LL, TPL and VL, respectively. As show in Fig. 8, the ratio of DB correlation predicted Nu and experimental Nu is very close to 1 in the LL and VL regimes, but deviates significantly from 1 in the TPL regime, indicating that SHT has significant multiphase feature in the TPL regime. A set of dimensionless parameters are defined for TPL regime to reflect the mass, momentum and energy interactions between LL phase and VL phase. Future work such as experimental methodologies and numerical simulations were also suggested for emphasizing the multiphase feature of SFs.

Summary and outlook

This paper presents a critical review on the heat transfer of SFs, summarizing the existing literature for SHT, including SFs heated in tubes, SFs cooled in tubes, and the newly emerged concept of supercritical pseudo-boiling. Although SHT has been extensively studied in the past several decades with numerous publications reporting important discoveries using a variety of methods, there are still issues remained elusive, and future efforts are needed to enable thorough

understanding and accurate prediction of SHT.

The existing experimental studies for both water and CO_2 are mostly focusing on near critical conditions, and the working pressures are within narrow ranges. Experiments with broader ranges of working parameters are recommended to be carried out, to provide sufficient experimental data for better understanding of the heat transfer characteristics. More complex working conditions, such as non-uniform heating, various inclination angles, and different tube geometries such as semi-circular and structured tubes (grooved, coiled, dimpled, etc.), should be investigated. Moreover, compared with the abundant experimental results for heating of SFs, supercritical cooling heat transfer is not extensively studies, and existing publications mostly focused on narrow parameter ranges. More comprehensive experimental investigations should be conducted to provide sufficient data for analysis. In particular, a more universal heat transfer correlation should be developed.

The pseudo-boiling concept shows successful application in describing SHT, but only limited works have been reported so far. Based on the analogy between subcritical boiling and supercritical pseudo-boiling, more efforts can be made to transfer the experimental and numerical methodologies for subcritical boiling into supercritical pseudo-boiling [174]. For example, Tripathi and Basu [175] applied the volume of fluid multiphase model to numerically study supercritical pseudo-boiling, showing good agreement with experiments.

Through MD simulations, Tamba et al. [176] found that a finite value of surface tension exists even in supercritical pressures, when the SF is subject to a temperature gradient. The results also

indicate that the surface tension at the LL-GL interface greatly influence SHT. Unfortunately, no further studies have been reported regarding the surface tension in SFs. Therefore, the concept of supercritical surface tension should also be further investigated both theoretically and experimentally. Since surface tension is very important for multiphase flow, the knowledge about supercritical surface tension will fill the gap in the multiphase framework proposed by Ref. [174], and provide substantial opportunities for analyzing and understanding SHT in the future.

Nomenclature

Ac	non-dimensional flow acceleration parameter
Bo	boiling number
Bu, Bu^*	buoyancy parameter
c_p	specific heat capacity, J/(kg·K)
DNS	direct numerical simulation
d_{in}	inner tube diameter, m
Fr	Froude number
f	friction factor
G	mass flux, kg/m^{2}s
Gr, Gr_q, Gr_g, Gr^*	Grashof number
GL	gas-like
g	gravitational acceleration, m/s^2

HTC	heat transfer coefficient, W/m^2K
HTD	heat transfer deterioration
HTE	heat transfer enhancement
i	enthalpy, J/kg
K	supercritical K number
K_v, $K_{v,T}$, $K_{v,P}$	flow acceleration parameters
L	heating length, mm
LES	large eddy simulation
LL	liquid-like
MD	molecular dynamics
NHT	normal heat transfer
Nu	Nusselt number
PCHE	printed circuit heat exchanger
P	pressure, Pa
P_c	critical pressure, Pa
Pr	Prandtl number
q^+	non-dimensional heat flux
q_w	wall heat flux, W/m^2
RNG	renormalization group
Re	Reynolds number

SBO	supercritical boiling number
SF	supercritical fluid
SHT	supercritical heat transfer
T	temperature, K or °C
TPL	two-phase-like
VL	vapor-like (same meaning as gas-like)
x	pseudo-vapor mass quality

Greek symbols

α_T	isothermal compressibility, 1/Pa
α_p	volumetric expansion coefficient, 1/T
β	volumetric expansivity, 1/K
β_T	volumetric compression coefficient, 1/Pa
ΔT	temperature difference, K
λ	thermal conductivity, W/m K
μ	dynamic viscosity, Pa·s
v	kinematic viscosity, m^2/s
ρ	density, kg/m^3

Subscripts

ave	average
b	bulk fluid
bottom	bottom generatrix
CHF	critical heat flux
c	critical point
cr	critical value
DB	Dittus-Boelter correlation
FC	forced convection
f	film temperature condition
pc	pseudo-critical point
r	reduced value
top	top generatrix
w	inner wall condition

Acknowledgements

This work is supported by the National Natural Science Foundation of China (Grant No. 52106198 and 52130608).

References

[1] Ž. Knez et al., "Industrial applications of supercritical fluids: A review," *Energy*, vol. 77, pp. 235-243, 2014. DOI:10.1016/j.energy.2014.07.044.

[2] E. Ramsey, Q. Sun, Z. Zhang, C. Zhang, and W. Gou, "Mini-Review: green sustainable processes using supercritical fluid carbon dioxide," *J. Environ. Sci*., vol. 21, no. 6, pp. 720-726, 2009. DOI:10.1016/S1001-0742(08)62330-X.

[3] L. Guo, H. Jin, and Y. Lu, "Supercritical water gasification research and development in China," *J. Supercrit. Fluid*, vol. 96, no. pp. 144-150, 2015. DOI:10.1016/j.supflu.2014.09.023.

[4] Z. Shengxuan et al., "Supercritical fluid drying: classification and applications," *Recent. Pat. Chem. Eng.*, vol. 3, no. 3, pp. 230-244, 2010. DOI: 10.2174/2211334711003030230.

[5] Ž. Knez, M. Škerget, and M. KnezHrnčič, "Principles of supercritical fluid extraction and applications in the food, beverage and nutraceutical industries, in: separation, extraction and concentration processes in the food," Beverage and Nutraceutical Industries, 2010, pp. 3-38. DOI: 10.1533/9780857090751.1.3.

[6] L. Qian et al., "Treatment of municipal sewage sludge in supercritical water: A review," *Water Res.*, vol. 89, pp. 118-131, 2016. DOI:10.1016/j.watres.2015.11.047.

[7] J. Xu et al., "Perspective of sCO_2 power cycles," *Energy*, vol. 186, pp. 115831, 2019. DOI: 10.1016/j.energy.2019.07.161.

[8] J. Xu, E. Sun, M. Li, H. Liu, and B. Zhu, "Key issues and solution strategies for supercritical carbon dioxide coal fired power plant," *Energy,* vol. 157, pp. 227-246, 2018. DOI:

10.1016/j.energy.2018.05.162.

[9] L. Chai and S.A. Tassou, "Modeling and evaluation of the thermohydraulic performance of compact recuperative heat exchangers in supercritical carbon dioxide waste heat to power conversion systems," *Heat Transf. Eng.*, vol. 43, no. 13, pp. 1067-1082, 2022. DOI: 10.1080/01457632.2021.1943833.

[10] E. Schroder, K. Neumaier, F. Nagel, and C. Vetter, "Study on heat transfer in heat exchangers for a new supercritical organic Rankine cycle," *Heat Transf. Eng.*, vol. 38, no. 18, pp. 1505-1519, 2014. DOI: 10.1080/01457632.2014.897558.

[11] G. Lorentzen, and J. Pettersen, "A new, efficient and environmentally benign system for car air-conditioning," *Int. J. Refrig.*, vol. 16, no. 1, pp. 4-12, 1993. DOI: 10.1016/0140-7007(93)90014-Y.

[12] B. Yu, J. Yang, D. Wang, J. Shi, and J. Chen, "An updated review of recent advances on modified technologies in transcritical CO_2 refrigeration cycle," *Energy*, vol. 189, pp. , 2019. DOI: 10.1016/j.energy.2019.116147.

[13] J.M. Han et al., "Off-design analysis of a supercritical CO_2 Brayton cycle with ambient air as the cold source driven by waste heat from gas turbine," *Heat Transf. Eng.*, vol. 42, no. 16, pp. 1321-1331, 2021. DOI: 10.1080/01457632.2020.1794620.

[14] H. Zhang et al., "Experimental and numerical investigations of thermal-hydraulic characteristics in a novel airfoil fin heat exchanger, " *Int. J. Heat Mass Transf.*, vol. 175, pp. 121333, 2021. DOI: 10.1016/j.ijheatmasstransfer.2021.121333.

[15] W.-X. Chu, X.-H. Li, T. Ma, Y.-T. Chen, and Q.-W. Wang, "Experimental investigation on sCO$_2$-water heat transfer characteristics in a printed circuit heat exchanger with straight channels," *Int. J. Heat Mass Transf.*, vol. 113, pp. 184-194, 2017. DOI: 10.1016/j.ijheatmasstransfer.2017.05.059.

[16] Z.R. Peng, Q.Y. Zheng, and X.R. Zhang, "Numerical study of condensation process in semi-circular mini-channels for the printed circuit heat exchanger," *Heat Transf. Eng.*, vol. 43, no. 8-10, pp. 785-793, 2022. DOI: 10.1080/01457632.2021.1905322.

[17] T. Ishizuka, Y. Kato, Y. Muto, K. Nikiti, and N. Lam, "Thermal-hydraulic characteristics of a printed circuit heat exchanger in a supercritical CO_2 loop," *Bull. Res. Lab. Nucl. React.*, vol. 30, pp. 109-116, 2006.

[18] Z. Ren, L. Zhang, C.R. Zhao, P.X. Jiang, and H.L. Bo, "Local flow and heat transfer of supercritical CO_2 in semicircular zigzag channels of printed circuit heat exchanger during cooling," *Heat Transf. Eng.*, vol. 42, no. 22, pp. 1889-1913, 2021. DOI: 10.1080/01457632.2020.1834205.

[19] L.H. Tang, B.H. Yang, J. Pan, and B. Sunden, "Thermal performance analysis in a zigzag channel printed circuit heat exchanger under different conditions" *Heat Transf. Eng.*, vol. 43, no. 7, pp. 567-583, 2022. DOI: 10.1080/01457632.2021.1896832.

[20] S.M. Lee, and K.Y. Kim, "A parametric study of the thermal-hydraulic performance of a zigzag printed circuit heat exchanger," *Heat Transf. Eng.*, vol.35, no. 13, pp. 1192-1200, 2014. DOI: 10.1080/01457632.2013.870004.

[21] T.L. Ngo, Y.Kato, K. Nikitin, and N. Tsuzuki, "New printed circuit heat exchanger with s-shaped fins for hot water supplier," *Exp. Therm. Fluid Sci.*, vol. 30, no. 8, pp. 811-819, 2006. DOI: 10.1016/j.expthermflusci.2006.03.010.

[22] D.E. Kim, M.H. Kim, J.E. Cha, and S.O. Kim, "Numerical investigation on thermal–hydraulic performance of new printed circuit heat exchanger model," *Nucl. Eng. Des.*, vol. 238, no. 12, pp. 3269-3276, 2008. DOI: 10.1016/j.nucengdes.2008.08.002.

[23] W.-X. Chu, K. Bennett, J. Cheng, Y.-T. Chen, and Q.-W. Wang, "Thermo-hydraulic performance of printed circuit heat exchanger with different cambered airfoil fins," *Heat Transf. Eng.*, vol. 41, no. 8, pp. 708-722, 2020. DOI: 10.1080/01457632.2018.1564203.

[24] L.H. Tang, J. Pan, and B. Sunden, "Investigation on thermal-hydraulic performance in a printed circuit heat exchanger with airfoil and vortex generator fins for supercritical liquefied natural gas," *Heat Transf. Eng.*, vol. 42, no. 10, pp. 802-823, 2021. DOI: 10.1080/01457632.2020.1744244.

[25] G. Kuang, M. Ohadi, and Y. Zhao, "Experimental study on gas cooling heat transfer for supercritical CO_2 in microchannels," ASME 2nd Int. Conference on Microchannels and Minichannels, New York, USA, June 17-19, 2004. pp. 325-332. DOI: 10.1115/ICMM2004-2352.

[26] X.L. Huai, S. Koyama, and T.S. Zhao, "An experimental study of flow and heat transfer of supercritical carbon dioxide in multi-port mini channels under cooling conditions," *Chem. Eng. Sci.*, vol. 60, no. 12, pp. 3337-3345, 2005. DOI: 10.1016/j.ces.2005.02.039.

[27] X. Huai, and S. Koyama, "Heat transfer characteristics of supercritical CO_2 flow in small-

channeled structures," *Exp. Heat Transf.*, vol. 20, no. 1, pp. 19-33, 2007.

[28] H. Wang, L.K. Leung, W. Wang, and Q. Bi, "A review on recent heat transfer studies to supercritical pressure water in channels," *Appl. Therm. Eng.*, vol. 142, pp. 573-596, 2018. DOI: 10.1016/j.applthermaleng.2018.07.007.

[29] I.L. Pioro, and R.B. Duffey, "Experimental heat transfer in supercritical water flowing inside channels (survey)," *Nucl. Eng. Des.*, vol. 235, no. 22, pp. 2407-2430, 2005. DOI:10.1016/j.nucengdes.2005.05.034.

[30] M.M. Ehsan, Z. Guan, and A. Klimenko, "A comprehensive review on heat transfer and pressure drop characteristics and correlations with supercritical CO_2 under heating and cooling applications," *Renew. Sust. Energ. Rev.*, vol. 92, pp. 658-675, 2018. DOI: 10.1016/j.rser.2018.04.106.

[31] R.B. Duffey, and I.L. Pioro, "Experimental heat transfer of supercritical carbon dioxide flowing inside channels (survey)," *Nucl. Eng. Des.*, vol. 235, no. 8, pp. 913-924, 2005. DOI:10.1016/j.nucengdes.2004.11.011.

[32] L.F. Cabeza, A. de Gracia, A.I. Fernández, and M.M. Farid, "Supercritical CO_2 as heat transfer fluid: a review," *Appl. Therm. Eng.*, vol. 125, pp. 799-810, 2017. DOI:10.1016/j.applthermaleng.2017.07.049.

[33] D.E. Kim, and M.H. Kim, "Experimental investigation of heat transfer in vertical upward and downward supercritical CO_2 flow in a circular tube," *Int. J. Heat Fluid Flow*, vol. 32, no. 1, pp. 176-191, 2011. DOI: 10.1016/j.ijheatfluidflow.2010.09.001.

[34] S. Gupta et al., "Developing empirical heat-transfer correlations for supercritical CO_2 flowing in vertical bare tubes," *Nucl. Eng. Des.*, vol. 261, pp. 116-131, 2013. DOI: 10.1016/j.nucengdes.2013.02.048.

[35] P.-X. Jiang, B. Liu, C.-R. Zhao, and F. Luo, "Convection heat transfer of supercritical pressure carbon dioxide in a vertical micro tube from transition to turbulent flow regime," *Int. J. Heat Mass Transf.*, vol. 56, no. 1, pp. 741-749, 2013. DOI:10.1016/j.ijheatmasstransfer.2012.08.038.

[36] K. Tanimizu, and R. Sadr, "Experimental investigation of buoyancy effects on convection heat transfer of supercritical CO_2 flow in a horizontal tube, " *Heat Mass Transf.*, vol. 52, no. 4, pp. 713-726, 2016. DOI: 10.1007/s00231-015-1580-9.

[37] S. Liu, Y. Huang, G. Liu, J. Wang, and L.K.H. Leung, "Improvement of buoyancy and acceleration parameters for forced and mixed convective heat transfer to supercritical fluids flowing in vertical tubes," *Int. J. Heat Mass Transf.*, vol. 106, pp. 1144-1156, 2017. DOI: 10.1016/j.ijheatmasstransfer.2016.10.093.

[38] H. Zahlan, D. Groeneveld, and S. Tavoularis," Measurements of convective heat transfer to vertical upward flows of CO_2 in circular tubes at near-critical and supercritical pressures," *Nucl. Eng. Des.*, vol. 289, pp. 92-107, 2015. DOI: 10.1016/j.nucengdes.2015.04.013.

[39] Q. Zhang, H. Li, X. Kong, J. Liu, and X. Lei, "Special heat transfer characteristics of supercritical CO_2 flowing in a vertically-upward tube with low mass flux," *Int. J. Heat Mass Transf.*, vol. 122, pp. 469-482, 2018. DOI: 10.1016/j.ijheatmasstransfer.2018.01.112.

[40] B. Zhu, J. Xu, X. Wu, J. Xie, and M. Li, "Supercritical “boiling” number, a new parameter to

distinguish two regimes of carbon dioxide heat transfer in tubes," *Int. J. Therm. Sci.*, vol. 136, pp. 254-266, 2019. DOI: 10.1016/j.ijthermalsci.2018.10.032.

[41] P. Guo, S. Liu, J. Yan, J. Wang, and Q. Zhang, "Transfer, Experimental study on heat transfer of supercritical CO_2 flowing in a mini tube under heating conditions," *Int. J. Heat Mass Transf.,* vol. 153, pp. 119623, 2020. DOI: 10.1016/j.ijheatmasstransfer.2020.119623.

[42] L. Wang et al., "Experimental investigation in the local heat transfer of supercritical carbon dioxide in the uniformly heated horizontal miniature tubes," *Int. J. Heat Mass Transf.*, vol. 159, pp. 120136, 2020. DOI: 10.1016/j.ijheatmasstransfer.2020.120136.

[43] H. Zhang, J. Xu, Q. Wang, and X. Zhu," Multiple wall temperature peaks during forced convective heat transfer of supercritical carbon dioxide in tubes," *Int. J. Heat Mass Transf.*, vol. 172, pp. 121171, 2021. DOI: 10.1016/j.ijheatmasstransfer.2021.121171.

[44] X. Zhu, Q. Bi, D. Yang, and T. Chen, "An investigation on heat transfer characteristics of different pressure steam-water in vertical upward tube," *Nucl. Eng. Des.*, vol. 239, no. 2, pp. 381-388, 2009. DOI: 10.1016/j.nucengdes.2008.10.026.

[45] S. Mokry et al., "Development of supercritical water heat-transfer correlation for vertical bare tubes," *Nucl. Eng. Des.*, vol. 241, no. 4, pp. 1126-1136, 2011. DOI: 10.1016/j.nucengdes.2010.06.012.

[46] G. Zhang, H. Zhang, H. Gu, Y. Yang, and X. Cheng, "Experimental and numerical investigation of turbulent convective heat transfer deterioration of supercritical water in vertical tube," *Nucl. Eng. Des.*, vol. 248, pp. 226-237, 2012. DOI: 10.1016/j.nucengdes.2012.03.026.

[47] S. Yu et al., "Experimental investigation on heat transfer characteristics of supercritical pressure water in a horizontal tube," *Exp. Therm. Fluid Sci.*, vol. 50, pp. 213-221, 2013. DOI: 10.1016/j.expthermflusci.2013.06.011.

[48] S. Yu et al., "Influence of buoyancy on heat transfer to water flowing in horizontal tubes under supercritical pressure," *Appl. Therm. Eng.*, vol. 59, no. 1, pp. 380-388, 2013. DOI: 10.1016/j.applthermaleng.2013.05.034.

[49] Z. Shen, D. Yang, G. Chen, and F. Xiao, "Experimental investigation on heat transfer characteristics of smooth tube with downward flow," *Int. J. Heat Mass Transf.*, vol. 68, pp. 669-676, 2014. DOI: 10.1016/j.ijheatmasstransfer.2013.09.045.

[50] H.Y. Gu, M. Zhao, and X. Cheng, "Experimental studies on heat transfer to supercritical water in circular tubes at high heat fluxes," *Int. J. Therm. Sci.*, vol. 65, pp. 22-32, 2015. DOI: 10.1016/j.expthermflusci.2015.03.001.

[51] Z. Shen et al., "Flow and heat transfer characteristics of high-pressure water flowing in a vertical upward smooth tube at low mass flux conditions," *Appl. Therm. Eng.*, vol. 102, pp. 391-401, 2016. DOI: 10.1016/j.applthermaleng.2016.03.150.

[52] X. Lei et al., "Experimental study on the difference of heat transfer characteristics between vertical and horizontal flows of supercritical pressure water," *Appl. Therm. Eng.*, vol. 113, pp. 609-620, 2017. DOI: 10.1016/j.applthermaleng.2016.11.051.

[53] J. Xu, and T. Chen, "A nonlinear solution of inverse heat conduction problem for obtaining the inner heat transfer coefficient," *Heat Transf. Eng.*, vol. 19, no. 2, pp. 45-53, 1998. DOI:

10.1080/01457639808939920.

[54] X. Lei, Q. Zhang, J. Zhang, and H. Li, "Experimental and numerical investigation of convective heat transfer of supercritical carbon dioxide at low mass fluxes," *Appl. Sci.*, vol. 7, no. 12, pp. 1260, 2017. DOI: 10.3390/app7121260.

[55] J. Ackerman, "Pseudoboiling heat transfer to supercritical pressure water in smooth and ribbed tubes," *J. Heat Transfer*, vol. 92, no. 3, pp. 490-497, 1970. DOI: 10.1115/1.3449699.

[56] B. Shiralkar, and P. Griffith, "Deterioration in heat transfer to fluid at supercritical pressure and high heat flux," Massachusetts Inst. of Tech., Cambridge. Dept. of Mechanical Engineering, 1968. DOI: 10.2172/4500456.

[57] P.-X. Jiang, Y. Zhang, Y.-J. Xu, and R.-F. Shi, "Experimental and numerical investigation of convection heat transfer of CO_2 at supercritical pressures in a vertical tube at low Reynolds numbers," *Int. J. Therm. Sci.*, vol. 47, no. 8, pp. 998-1011, 2008. DOI:10.1016/j.ijthermalsci.2007.08.003.

[58] M. Zhao, H. Gu, and X. Cheng, "Experimental study on heat transfer of supercritical water flowing downward in circular tubes," *Ann. Nucl. Energy*, vol. 63, pp. 339-349, 2014. DOI: 10.1016/j.anucene.2013.07.003.

[59] D. Huang, Z. Wu, B. Sunden, and W. Li, "A brief review on convection heat transfer of fluids at supercritical pressures in tubes and the recent progress," *Appl. Energy*, vol. 162, pp. 494-505, 2016. DOI:10.1016/j.apenergy.2015.10.080.

[60] I.L. Pioro, H.F. Khartabil, and R.B. Duffey, "Heat transfer to supercritical fluids flowing in

channels—empirical correlations (survey)," *Nucl. Eng. Des*, vol. 230, no. 1-3, pp. 69-91, 2004. DOI: 10.1016/j.nucengdes.2003.10.010.

[61] H.S. Swenson, J.R. Carver, and C.R. Kakarala, "Heat transfer to supercritical water in smooth-bore tubes," *J. Heat Transfer.*, vol. 87, no. 4, pp. 477-483, 1965. DOI:10.1115/1.3689139.

[62] G. Liu, Y. Huang, J. Wang, and L.H. Leung, "Heat transfer of supercritical carbon dioxide flowing in a rectangular circulation loop," *Appl. Therm. Eng.*, vol. 98, pp. 39-48, 2016. DOI: 10.1016/j.applthermaleng.2015.11.110.

[63] J. Wang et al., "Investigation of forced convection heat transfer of supercritical pressure water in a vertically upward internally ribbed tube," *Nucl. Eng. Des*., vol. 239, no. 10, pp. 1956-1964, 2009. DOI: 10.1016/j.nucengdes.2009.04.012.

[64] S. Yildiz, and D. Groeneveld, "Diameter effect on supercritical heat transfer," *Int. Commun. Heat Mass Transf.*, vol. 54, pp. 27-32, 2014. DOI: 10.1016/j.icheatmasstransfer.2014.02.017.

[65] J. Song, H. Kim, H. Kim, and Y. Bae, "Heat transfer characteristics of a supercritical fluid flow in a vertical pipe," *J. Supercrit. Fluids*, vol. 44, no. 2, pp. 164-171, 2008. DOI: 10.1016/j.supflu.2007.11.013.

[66] Y.-Y. Bae, H.-Y. Kim, and D.-J. Kang, "Forced and mixed convection heat transfer to supercritical CO_2 vertically flowing in a uniformly-heated circular tube," *Exp. Therm. Fluid Sci.*, vol. 34, no. 8, pp. 1295-1308, 2010. DOI: 10.1016/j.expthermflusci.2010.06.001.

[67] Y.Y. Bae, "Mixed convection heat transfer to carbon dioxide flowing upward and downward in a vertical tube and an annular channel," *Nucl. Eng. Des.,* vol. 241, no. 8, pp. 3164-3177, 2011.

DOI: 10.1016/j.nucengdes.2011.06.016.

[68] T. Yamashita et al., "Heat transfer study under supercritical pressure conditions," GENE4/ANP2003, Paper, vol. 1119, pp. 2003.

[69] P. Bourke, D. Pulling, L. Gill, and W. Denton, "Forced convective heat transfer to turbulent CO_2 in the supercritical region," *Int. J. Heat Mass Transf.*, vol. 13, no. 8, pp. 1339-1348, 1970. DOI: 10.1016/0017-9310(70)90074-8.

[70] Z.-H. Li, P.-X. Jiang, C.-R. Zhao, and Y. Zhang, "Experimental investigation of convection heat transfer of CO_2 at supercritical pressures in a vertical circular tube," *Exp. Therm. Fluid Sci.*, vol. 34, no. 8, pp. 1162-1171, 2010. DOI: 10.1016/j.expthermflusci.2010.04.005.

[71] J. Fewster, "Mixed forced and free convective heat transfer to supercritical pressure fluids flowing in vertical pipes," The University of Manchester, 1976.

[72] S.M. Liao, and T.S. Zhao, "An experimental investigation of convection heat transfer to supercritical carbon dioxide in miniature tubes," *Int. J. Heat Mass Transf.*, vol. 45, no. 25, pp. 5025-5034, 2002. DOI:10.1016/S0017-9310(02)00206-5.

[73] P.-X. Jiang, Y. Zhang, C.-R. Zhao, and R.-F. Shi, "Convection heat transfer of CO_2 at supercritical pressures in a vertical mini tube at relatively low Reynolds numbers," *Exp. Therm. Fluid Sci.*, vol. 32, no. 8, pp. 1628-1637, 2008. DOI: 10.1016/j.expthermflusci.2008.05.006.

[74] G.A. Adebiyi, and W. Hall, "Experimental investigation of heat transfer to supercritical pressure carbon dioxide in a horizontal pipe," *Int. J. Heat Mass Transf.*, vol. 19, no. 7, pp. 715-720, 1976. DOI: 10.1016/0017-9310(76)90123-X.

[75] T.H. Kim, J.G. Kwon, M.H. Kim, and H.S. Park, "Experimental investigation on validity of buoyancy parameters to heat transfer of CO_2 at supercritical pressures in a horizontal tube," *Exp. Therm. Fluid Sci.*, vol. 92, pp. 222-230, 2018. DOI: 10.1016/j.expthermflusci.2017.11.024.

[76] B. Shiralkar, and P. Griffith, "The effect of swirl, inlet conditions, flow direction, and tube diameter on the heat transfer to fluids at supercritical pressure," *J. Heat Transf.*, vol. 92, no. 3, pp. 465-471, 1970. DOI: 10.1115/1.3449690.

[77] J.D. Jackson, and W.B. Hall, "Influences of buoyancy on heat transfer to fluids flowing in vertical tubes under turbulent conditions," Institution of Mechanical Engineers, Conference Publications, vol. 2, pp. 613-640, 1979.

[78] H. Deng, K. Zhu, G. Xu, Z. Tao, and J. Sun, "Heat transfer characteristics of RP-3 kerosene at supercritical pressure in a vertical circular Tube," *J. Enhanc. Heat Transf.* vol. 19, no. 5, pp. 409-421, 2012. DOI: 10.1615/JEnhHeatTransf.2012004966.

[79] T. Hiroaki, T. Ayao, H. Masaru, and N. Nuchi, "Effects of buoyancy and of acceleration owing to thermal expansion on forced turbulent convection in vertical circular tubes—criteria of the effects, velocity and temperature profiles, and reverse transition from turbulent to laminar flow," *Int. J. Heat Mass Transf.*, vol.16, no. 6, pp. 1267-1288, 1973. DOI: doi.org/10.1016/0017-9310(73)90135-X.

[80] J. Jackson, M. Cotton, and B. Axcell, "Studies of mixed convection in vertical tubes," *Int. J. Heat Fluid Flow*, vol. 10, no. 1, pp. 2-15, 1989. DOI: 10.1016/0142-727X(89)90049-0.

[81] D.E. Kim, and M.H. Kim, "Experimental study of the effects of flow acceleration and

buoyancy on heat transfer in a supercritical fluid flow in a circular tube," *Nucl. Eng. Des.*, vol. 240, no. 10, pp. 3336-3349, 2010. DOI: doi.org/10.1016/j.nucengdes.2010.07.002.

[82] G. Liu, Y. Huang, J. Wang, and F. Lv, "Effect of buoyancy and flow acceleration on heat transfer of supercritical CO_2 in natural circulation loop," *Int. J. Heat Mass Transf.*, vol.91, pp. 640-646, 2015. DOI: 10.1016/j.ijheatmasstransfer.2015.08.009.

[83] V. Protopopov, "Generalizing relations for the local heat-transfer coefficients in turbulent flows of water and carbon dioxide at supercritical pressure in a uniformly heated circular tube," *Teplofizika Vysokikh Temp.*, vol. 15, pp. 815-821, 1977.

[84] K.W. Seo, M.H. Kim, M.H. Anderson, and M.L. Corradini, "Heat transfer in a supercritical fluid: classification of heat transfer regimes," *Nucl. Technol.*, vol. 154, no. 3, pp. 335-349, 2006. DOI: doi.org/10.13182/NT06-A3738.

[85] B. Petukhov, A. Polyakov, V. Kuleshov, and Y. Sheckter, "Turbulent flow and heat transfer in horizontal tubes with substantial influence of thermogravitational forces," presented at the 5th Int. Heat Transf. Conf., Tokyo, Japan, Sept. 3-7, 1974. pp. 164-168. DOI: 10.1615/IHTC5.3130.

[86] H. Gu, H. Li, H. Wang, and Y. Luo, "Experimental investigation on convective heat transfer from a horizontal miniature tube to methane at supercritical pressures," *Appl. Therm. Eng.*, vol. 58, no. 1, pp. 490-498, 2013. DOI: doi.org/10.1016/j.applthermaleng.2013.04.049.

[87] D. McEligot, C. Coon, and H. Perkins, "Relaminarization in tubes," *Int. J. Heat Mass Transf.*, vol. 13, no. 2, pp. 431-433, 1970. DOI:10.1016/0017-9310(70)90118-3.

[88] D. Huang, and W. Li, "A brief review on the buoyancy criteria for supercritical fluids," *Appl.*

Therm. Eng., vol. 131, pp. 977-987, 2018. DOI: 10.1016/j.applthermaleng.2017.12.042.

[89] D.M. McEligot, and J.D. Jackson, "Deterioration' criteria for convective heat transfer in gas flow through non-circular ducts," *Nucl. Eng. Des.*, vol. 232, no. 3, pp. 327-333, 2004. DOI:10.1016/j.nucengdes.2004.05.004.

[90] C.-R. Zhao, Z. Zhang, P.-X. Jiang, R.-N. Xu, and H.-L. Bo, "Influence of channel scale on the convective heat transfer of CO_2 at supercritical pressure in vertical tubes," *Int. J. Heat Mass Transf.*, vol. 126, pp. 201-210, 2018. DOI:10.1016/j.ijheatmasstransfer.2018.04.080.

[91] Q. Zhang, H. Li, X. Lei, J. Zhang, and X. Kong, "Study on identification method of heat transfer deterioration of supercritical fluids in vertically heated tubes," *Int. J. Heat Mass Transf.*, vol. 127, pp. 674-686, 2018. DOI:10.1016/j.ijheatmasstransfer.2018.07.058.

[92] Z. Luo, X. Fang, Y. Yang, W. Chen, and L. Zhang, "Prediction of “critical heat flux” for supercritical water and CO_2 flowing upward in vertical heated tubes," *Int. J. Heat Mass Transf.*, vol. 159, pp. 120115, 2020. DOI: 10.1016/j.ijheatmasstransfer.2020.120115.

[93] J. Xu, H. Zhang, B. Zhu, and J. Xie, "Critical supercritical-boiling-number to determine the onset of heat transfer deterioration for supercritical fluids," *Sol. Energy*, vol. 195, pp. 27-36, 2020. DOI: 10.1016/j.solener.2019.11.036.

[94] Y.-Y. Bae, and H.-Y. Kim, "Convective heat transfer to CO_2 at a supercritical pressure flowing vertically upward in tubes and an annular channel," *Exp. Therm. Fluid Sci*., vol. 33, no. 2, pp. 329-339, 2009. DOI: 10.1016/j.expthermflusci.2008.10.002.

[95] J.D. Jackson, "Fluid flow and convective heat transfer to fluids at supercritical pressure," *Nucl.*

Eng. Des. , vol. 264, pp. 24-40, 2013. DOI: 10.1016/j.nucengdes.2012.09.040.

[96] A.A. Bishop, R.O. Sandberg, and L.S. Tong, "Forced convection heat transfer to water at near-critical temperatures and supercritical pressures," *AIChEI Chem e Symposium Series No 2*, vol. 2, pp. 77-85, 1964.

[97] J. Yu, B. Jia, D. Wu, and D. Wang, "Optimization of heat transfer coefficient correlation at supercritical pressure using genetic algorithms," *Heat Mass Transf.*, vol. 45, pp. 757-766, 2009. DOI: 10.1007/s00231-008-0475-4.

[98] B. Zhu, J. Xu, C. Yan, and J. Xie, "The general supercritical heat transfer correlation for vertical up-flow tubes: K number correlation," *Int. J. Heat Mass Transf.*, vol. 148, pp. 119080, 2020. DOI: 10.1016/j.ijheatmasstransfer.2019.119080.

[99] F. Li, and B. Bai, "A model of heat transfer coefficient for supercritical water considering the effect of heat transfer deterioration," *Int. J. Heat Mass Transf.*, vol. 133, pp. 316-329, 2019. DOI:10.1016/j.ijheatmasstransfer.2018.12.121.

[100] J. Xie, D. Liu, H. Yan, G. Xie, and S.K. Boetcher, "A review of heat transfer deterioration of supercritical carbon dioxide flowing in vertical tubes: Heat transfer behaviors, identification methods, critical heat fluxes, and heat transfer correlations," *Int. J. Heat Mass Transf.*, vol. 149, pp. 119233, 2020. DOI: 10.1016/j.ijheatmasstransfer.2019.119233.

[101] K. Yamagata, K. Nishikawa, S. Hasegawa, T. Fujii, and S. Yoshida, "Forced convective heat transfer to supercritical water flowing in tubes," *Int. J. Heat Mass Transf.*, vol. 15, no. 12, pp. 2575-2593, 1972. DOI: 10.1016/0017-9310(72)90148-2.

[102] B. Zhang, J. Shan, and J. Jiang, "Numerical analysis of supercritical water heat transfer in horizontal circular tube," *Prog. Nucl. Energy*, vol. 52, no. 7, pp. 678-684, 2010. DOI: 10.1016/j.pnucene.2010.03.006.

[103] Z.-C. Wang, P.-X. Jiang, and R.-N. Xu, "Turbulent convection heat transfer analysis of supercritical pressure CO_2 flow in a vertical tube based on the field synergy principle," *Heat Transf. Eng.*, vol. 40, no. 5-6, pp. 476-486, 2019. DOI: 10.1080/01457632.2018.1432048.

[104] D. Palko, and H. Anglart, "Theoretical and numerical study of heat transfer deterioration in high performance light water reactor," *Sci. Technol. Nucl. Install.*, vol. 2008, pp. 405072, 2008. DOI: 10.1155/2008/405072.

[105] H. Wang, Q. Bi, Z. Yang, and L. Wang, "Experimental and numerical investigation of heat transfer from a narrow annulus to supercritical pressure water," *Ann. Nucl. Energy*, vol. 80, pp. 416-428, 2015. DOI:10.1016/j.anucene.2015.02.029.

[106] Q.L. Wen, and H.Y. Gu, "Numerical investigation of acceleration effect on heat transfer deterioration phenomenon in supercritical water," *Prog. Nucl. Energy*, vol. 53, no. 5, pp. 480-486, 2011. DOI: 10.1016/j.pnucene.2011.02.012.

[107] Q. Zhang, H. Li, J. Liu, X. Lei, and C. Wu, "Numerical investigation of different heat transfer behaviors of supercritical CO_2 in a large vertical tube," *Int. J. Heat Mass Transf.*, vol. 147, pp. 118944, 2020. DOI:10.1016/j.ijheatmasstransfer.2019.118944.

[108] Y.H. Fan, and G.H. Tang, "Numerical investigation on heat transfer of supercritical carbon dioxide in a vertical tube under circumferentially non-uniform heating," *Appl. Therm. Eng.*, vol.

138, pp. 354-364, 2018. DOI: 10.1016/j.applthermaleng.2018.04.060

[109] C. Yan, J. Xu, B. Zhu, and G. Liu, "Numerical analysis on heat transfer characteristics of supercritical CO_2 in heated vertical up-flow tube," *Materials*, vol. 13, no. 3, pp. 723, 2020. DOI: 10.3390/ma13030723.

[110] C. Yan, J. Xu, B. Zhu, X. He, and G. Liu, "Numerical study on convective heat transfer of supercritical CO_2 in vertically upward and downward tubes," *Sci. China: Technol. Sci.*, vol. 64, no. 5, pp. 995-1006, 2021. DOI: 10.1007/s11431-020-1773-9.

[111] M. Shitsman, "Impairment of the heat transmission at supercritical pressures(heat transfer process examined during forced motion of water at supercritical pressures)," *High Temp.*, vol. 1, pp. 237-244, 1963.

[112] A.P. Ornatskij, L.F. Glushchenko, and S.I. Kalachev, "Heat transfer with rising and falling flows of water in tubes of small diameter at supercritical pressures," *Therm. Eng.*, vol. 18, no. 5, pp. 137-141, 1971.

[113] K. Wang, X. Xu, Y. Wu, C. Liu, and C. Dang, "Numerical investigation on heat transfer of supercritical CO_2 in heated helically coiled tubes," *J. Supercrit. Fluids*, vol. 99 , pp. 112-120, 2015. DOI: 10.1016/j.supflu.2015.02.001.

[114] M. Mohseni, and M. Bazargan, "Effect of turbulent Prandtl number on convective heat transfer to turbulent flow of a supercritical fluid in a vertical round tube," *J. Heat Transf.*, vol. 133, no. 7, pp. 2011. DOI: 10.1115/1.4003570.

[115] Y.Y. Bae, "A new formulation of variable turbulent Prandtl number for heat transfer to

supercritical fluids," *Int. J. Heat Mass Transf.*, vol. 92, pp. 792-806, 2016. DOI: 10.1016/j.ijheatmasstransfer.2015.09.039.

[116] J. Xiong, and X. Cheng, "Turbulence modelling for supercritical pressure heat transfer in upward tube flow," *Nucl. Eng. Des.*, vol. 270, pp. 249-258, 2014. DOI: 10.1016/j.nucengdes.2014.01.014.

[117] F. Li, B. Pei, and B. Bai, "A non-linear turbulence model of supercritical fluid considering local non-equilibrium of Reynolds stress transport," *Phys. Fluids*, vol. 32, no. 9, pp. 095112, 2020. DOI: 10.1063/5.0020072.

[118] P.-X. Jiang, Z.-C. Wang, and R.-N. Xu, "A modified buoyancy effect correction method on turbulent convection heat transfer of supercritical pressure fluid based on RANS model," *Int. J. Heat Mass Transf.*, vol. 127, pp. 257-267, 2018. DOI: 10.1016/j.ijheatmasstransfer.2018.07.042.

[119] X. Du et al., "Heat transfer of supercritical CO_2 in vertical round tube: a considerate turbulent Prandtl number modification," *Energy*, vol. 192, pp. 116612, 2020. DOI: 10.1016/j.energy.2019.116612.

[120] R. Tian, X. Dai, D. Wang, and L. Shi, "Study of variable turbulent Prandtl number model for heat transfer to supercritical fluids in vertical tubes," *J. Therm. Sci*., vol. 27, no. 3, pp. 213-222, 2018. DOI: 10.1007/s11630-018-1002-7.

[121] G. Tang et al., "A variable turbulent Prandtl number model for simulating supercritical pressure CO_2 heat transfer," *Int. J. Heat Mass Transf.*, vol. 102, pp. 1082-1092, 2016. DOI: 10.1016/j.ijheatmasstransfer.2016.06.046.

[122] B. Ničeno, and M. Sharabi, "Large eddy simulation of turbulent heat transfer at supercritical pressures," *Nucl. Eng. Des.*, vol. 261, pp. 44-55, 2013. DOI: 10.1016/j.nucengdes.2013.03.042.

[123] F. Nicoud, and F. Ducros, "Subgrid-scale stress modelling based on the square of the velocity gradient tensor," *Flow, Turbul. Combust*., vol. 62, no. 3, pp. 183-200, 1999. DOI: 10.1023/A:1009995426001.

[124] J.H. Bae, J.Y. Yoo, and H. Choi, "Direct numerical simulation of turbulent supercritical flows with heat transfer," *Phys. Fluids*, vol. 17, no. 10, pp. 105104, 2005. DOI: 10.1063/1.2047588..

[125] X. Chu, and E. Laurien, "Flow stratification of supercritical CO_2 in a heated horizontal pipe," *J. Supercrit. Fluids*," vol. 116, pp. 172-189, 2016. DOI: 10.1016/j.supflu.2016.05.003.

[126] C. Dang, and E. Hihara, "In-tube cooling heat transfer of supercritical carbon dioxide. Part 1. experimental measurement," *Int. J. Refrig.*, vol. 27, no. 7, pp. 736-747, 2004. DOI: 10.1016/j.ijrefrig.2004.04.018.

[127] C.-H. Son, and S.-J. Park, "An experimental study on heat transfer and pressure drop characteristics of carbon dioxide during gas cooling process in a horizontal tube," *Int. J. Refrig.*, vol. 29, no. 4, pp. 539-546, 2006. DOI: 10.1016/j.ijrefrig.2005.10.010.

[128] H.-K. Oh, C.-H. Son, T.-G. Yu, and D.-H. Kim, "An experimental study on heat transfer and pressure drop characteristics of carbon dioxide during gas cooling process in a hellically coiled tube," *J. Korean Soc. Marine Eng.*, vol. 31, 2007. DOI: 10.5916/jkosme.2007.31.3.263.

[129] A. Bruch, A. Bontemps, and S. Colasson, "Experimental investigation of heat transfer of supercritical carbon dioxide flowing in a cooled vertical tube," *Int. J. Heat Mass Transf*., vol. 52,

no. 11, pp. 2589-2598, 2009. DOI: 10.1016/j.ijheatmasstransfer.2008.12.021.

[130] Z.-B. Liu, Y.-L. He, Y.-F. Yang, and J.-Y. Fei, "Experimental study on heat transfer and pressure drop of supercritical CO_2 cooled in a large tube," *Appl. Therm. Eng.*, vol. 70, no. 1, pp. 307-315, 2014. DOI: 10.1016/j.applthermaleng.2014.05.024.

[131] K.-Z. Wang, X.-X. Xu, C. Liu, W.-J. Bai, and C.-B. Dang, "Experimental and numerical investigation on heat transfer characteristics of supercritical CO_2 in the cooled helically coiled tube," *Int. J. Heat Mass Transf.*, vol. 108, pp. 1645-1655, 2017. DOI: 10.1016/j.ijheatmasstransfer.2017.01.004.

[132] G.-W. Zhang, P. Hu, L.-X. Chen, and M.-H. Liu, "Experimental and simulation investigation on heat transfer characteristics of in-tube supercritical CO_2 cooling flow," *Appli. Therm. Eng.*, vol. 143, pp. 1101-1113, 2018. DOI: 10.1016/j.applthermaleng.2018.07.108.

[133] X. Liu, X. Xu, C. Liu, J. He, and C. Dang, "The effect of geometry parameters on the heat transfer performance of supercritical CO_2 in horizontal helically coiled tube under the cooling condition," *Int. J. Refrig.*, vol. 106, pp. 650-661, 2019. DOI: 10.1016/j.ijrefrig.2019.02.008.

[134] Y. Lei, B. Xu, and Z. Chen, "Experimental investigation on cooling heat transfer and buoyancy effect of supercritical carbon dioxide in horizontal and vertical micro-channels," *Int. J. Heat Mass Transf.*, vol. 181, pp. 121792, 2021. DOI: 10.1016/j.ijheatmasstransfer.2021.121792.

[135] S. Liao, and T. Zhao, "Measurements of heat transfer coefficients from supercritical carbon dioxide flowing in horizontal mini/micro channels," *J. Heat Transfer*, vol. 124, no. 3, pp. 413-420, 2002. DOI: 10.1115/1.1423906.

[136] S.H. Yoon et al., "Heat transfer and pressure drop characteristics during the in-tube cooling process of carbon dioxide in the supercritical region," *Int. J. Refrig.*, vol. 26, no. 8, pp. 857-864, 2003. DOI: 10.1016/S0140-7007(03)00096-3.

[137] T. Ma, W.-X. Chu, X.-Y. Xu, Y.-T. Chen, and Q.-W. Wang, "An experimental study on heat transfer between supercritical carbon dioxide and water near the pseudo-critical temperature in a double pipe heat exchanger," *Int. J. Heat Mass Transf.*, vol. 93, pp. 379-387, 2016. DOI: 10.1016/j.ijheatmasstransfer.2015.10.017.

[138] H.-K. Oh, and C.-H. Son, "New correlation to predict the heat transfer coefficient in-tube cooling of supercritical CO_2 in horizontal macro-tubes," *Exp. Therm. Fluid Sci.*, vol. 34, no. 8, pp. 1230-1241, 2010. DOI: 10.1016/j.expthermflusci.2010.05.002.

[139] S.S. Pitla, E.A. Groll, and S. Ramadhyani, "New correlation to predict the heat transfer coefficient during in-tube cooling of turbulent supercritical CO_2," *Int. J. Refrig.*, vol. 25, no. 7, pp. 887-895, 2002. DOI: 10.1016/S0140-7007(01)00098-6.

[140] X. Fang, and Y. Xu, "Modified heat transfer equation for in-tube supercritical CO_2 cooling," *Appl. Therm. Eng.*, vol. 31, no. 14, pp. 3036-3042, 2011. DOI: 10.1016/j.applthermaleng.2011.05.037.

[141] L. Cheng, G. Ribatski, and J.R. Thome, "Analysis of supercritical CO_2 cooling in macro-and micro-channels," *Int. J. Refrig.*, vol. 31, no. 8, pp. 1301-1316, 2008. DOI: 10.1016/j.ijrefrig.2008.01.010.

[142] W. Lin, Z. Du, and A. Gu, "Analysis on heat transfer correlations of supercritical CO_2 cooled

in horizontal circular tubes," *Heat Mass Transf.*, vol. 48, no. 4, pp. 705-711, 2012. DOI: 10.1007/s00231-011-0919-0.

[143] S.S. Pitla, E.A. Groll, and S. Ramadhyani, "Convective heat transfer from in-tube flow of turbulent supercritical carbon dioxide: Part 1—numerical analysis," *HVAC Res.*, vol. 7, no. 4, pp. 345-366, 2001. DOI: 10.1080/10789669.2001.10391280.

[144] S. Liao, and T. Zhao, "A numerical investigation of laminar convection of supercritical carbon dioxide in vertical mini/micro tubes," *Prog. Comput. Fluid Dyn*., vol. 2, no. 2-4, pp. 144-152, 2002. DOI: 10.1504/PCFD.2002.003221.

[145] C. Dang, and E. Hihara, "In-tube cooling heat transfer of supercritical carbon dioxide. Part 2. comparison of numerical calculation with different turbulence models," *Int. J. Refrig*., vol. 27, no. 7, pp. 748-760, 2004. DOI: 10.1016/j.ijrefrig.2004.04.017.

[146] P.-X. Jiang, C.-R. Zhao, R.-F. Shi, Y. Chen, and W. Ambrosini, "Experimental and numerical study of convection heat transfer of CO_2 at super-critical pressures during cooling in small vertical tube," *Int. J. Heat Mass Transf.,* vol. 52, no. 21, pp. 4748-4756, 2009. DOI: 10.1016/j.ijheatmasstransfer.2009.06.014.

[147] Z. Du, W. Lin, and A. Gu, "Numerical investigation of cooling heat transfer to supercritical CO_2 in a horizontal circular tube," *J. Supercrit. Fluids*, vol. 55, no. 1, pp. 116-121, 2010. DOI: 10.1016/j.supflu.2010.05.023.

[148] X.L. Cao, Z.H. Rao, and S.M. Liao, "Laminar convective heat transfer of supercritical CO_2 in horizontal miniature circular and triangular tubes," *Appl. Therm. Eng.*, vol. 31, no. 14, pp. 2374-

2384, 2011. DOI: 10.1016/j.applthermaleng.2011.03.038.

[149] C. Yang, J. Xu, X. Wang, and W. Zhang, "Mixed convective flow and heat transfer of supercritical CO_2 in circular tubes at various inclination angles," *Int. J. Heat Mass Transf.*, vol. 64, pp. 212-223, 2013. DOI: 10.1016/j.ijheatmasstransfer.2013.04.033.

[150] H. Zhang, J. Guo, X. Huai, and X. Cui, "Thermodynamic performance analysis of supercritical pressure CO_2 in tubes," *Int. J. Therm. Sci*., vol. 146, pp. 106102, 2019. DOI: 10.1016/j.ijthermalsci.2019.106102.

[151] L. Diao, Y. Chen, and Y. Li, "Nonuniform heat transfer of supercritical pressure carbon dioxide under turbulent cooling condition in circular tubes at various inclination angles," *Nucl. Eng. Des*., vol. 352, pp. 110153, 2019. DOI: 10.1016/j.nucengdes.2019.110153.

[152] X. Wang, M. Xiang, H. Huo, and Q. Liu, "Numerical study on nonuniform heat transfer of supercritical pressure carbon dioxide during cooling in horizontal circular tube," *Appl. Therm. Eng.*, vol. 141, pp. 775-787, 2018. DOI: 10.1016/j.applthermaleng.2018.06.019.

[153] M. Xiang, J. Guo, X. Huai, and X. Cui, "Thermal analysis of supercritical pressure CO_2 in horizontal tubes under cooling condition," *J. Supercrit. Fluids*, vol. 130, pp. 389-398, 2017. DOI: 10.1016/j.supflu.2017.04.009.

[154] J. Guo et al., "Thermal-hydraulic characteristics of supercritical pressure CO_2 in vertical tubes under cooling and heating conditions," *Energy*, vol. 170, pp. 1067-1081, 2019. DOI: 10.1016/j.energy.2018.12.177.

[155] K. Goldmann, "Nuclear Development Corporation of America NDA-2-31," *Anal. Chem*., pp.

2-20, 1956. DOI: 10.1021/ac60146a736.

[156] J. Holman, S. Rea, and C. Howard, "Forced convection heat transfer to Freon 12 near the critical state in a vertical annulus," *Int. J. Heat Mass Transf.*, vol. 8, no. 8, pp. 1095-1102, 1965. DOI: 10.1016/0017-9310(65)90137-7.

[157] E. Stewart, P. Stewart, and A. Watson, "Thermo-acoustic oscillations in forced convection heat transfer to supercritical pressure water," *Int. J. Heat Mass Transf.,* vol. 16, no. 2, pp. 257-270, 1973. DOI: 10.1016/0017-9310(73)90055-0.

[158] N. Kafengauz, and M. Fedorov, "Excitation of high-frequency pressure oscillations during heat exchange with diisopropylcyclohexane," *J. Eng. Phys.*, vol. 11, no. 1, pp. 63-67, 1966. DOI: 10.1007/BF00829935.

[159] N. Kafengauz, and M. Fedorov, "Pseudoboiling and heat transfer in a turbulent flow," *J. Eng. Phys.*, vol. 14, no. 5, pp. 489-490, 1968. DOI: 10.1007/BF00828077.

[160] K. Sakurai, H. Ko, K. Okamoto, and H. Madarame, "Visualization study for forced convection heat transfer of supercritical carbon dioxide near pseudo-boiling point," *Trans. At. Energy Soc. Jpn*., 2001. DOI: 10.3327/taesj2002.3.34.2001.

[161] W. Ambrosini, "On the analogies in the dynamic behaviour of heated channels with boiling and supercritical fluids," *Nucl. Eng. Des.*, vol. 237, no. 11, pp. 1164-1174, 2007. DOI: 10.1016/j.nucengdes.2007.01.006.

[162] J. Tamba, T. Takahashi, T. Ohara, and T. Aihara, "Transition from boiling to free convection in supercritical fluid," *Exp. Therm. Fluid Sci.*, vol. 17, no. 3, pp. 248-255, 1998. DOI:

10.1016/S0894-1777(97)10062-0.

[163] G. Simeoni et al., "The Widom line as the crossover between liquid-like and gas-like behaviour in supercritical fluids," *Nat. Phys*., vol. 6, no. 7, pp. 503-507, 2010. DOI: 10.1038/nphys1683.

[164] P. Gallo, D. Corradini, and M. Rovere, "Widom line and dynamical crossovers as routes to understand supercritical water," *Nat. Commun.*, vol. 5, no. 1, pp. 1-6, 2014. DOI: 10.1038/ncomms6806.

[165] D. Banuti, "Crossing the Widom-line–supercritical pseudo-boiling," *J. Supercrit. Fluids*, vol. 98, pp. 12-16, 2015. DOI: 10.1016/j.supflu.2014.12.019.

[166] M.Y. Ha, T.J. Yoon, T. Tlusty, Y. Jho, and W.B. Lee, "Widom delta of supercritical gas–liquid coexistence," *J. Phys. Chem. Lett*., vol. 9, no. 7, pp. 1734-1738, 2018. DOI: 10.1021/acs.jpclett.8b00430.

[167] F. Maxim et al. "Visualization of supercritical water pseudo-boiling at Widom line crossover," *Nat. Commun.*, vol. 10, no. 1, pp. 1-11, 2019. DOI: 10.1038/s41467-019-12117-5.

[168] F. Maxim et al. "Thermodynamics and dynamics of supercritical water pseudo-boiling," *Adv. Sci*., vol. 8, no. 3, pp. 2002312, 2021. DOI: 10.1002/advs.202002312.

[169] J. Xu, Y. Wang, and X. Ma, "Phase distribution including a bubblelike region in supercritical fluid," *Phys. Rev. E.*, vol. 104, no. 1, pp. 014142, 2021. DOI:10.1103/PhysRevE.104.014142.

[170] S.G. Kandlikar, "Heat transfer mechanisms during flow boiling in microchannels," *J. Heat Transf.*, vol. 126, no. 1, pp. 8-16, 2004. DOI: 10.1115/ICMM2003-1005.

[171] S.G. Kandlikar, "Evaporation momentum force and its relevance to boiling heat transfer," *J. Heat Transf.*, vol. 142, no. 10, pp. 2020. DOI: 10.1115/1.4047268.

[172] B. Zhu, J. Xu, H. Zhang, J. Xie, and M. Li, "Effect of non-uniform heating on $scCO_2$ heat transfer deterioration," *Appl. Therm. Eng*., vol. 181, pp. 115967, 2020. DOI: 10.1016/j.applthermaleng.2020.115967.

[173] H. Zhang et al., "The K number, a new analogy criterion number to connect pressure drop and heat transfer of sCO_2 in vertical tubes," *Appl. Therm. Eng*., vol. 182, pp. 116078, 2021. DOI: 10.1016/j.applthermaleng.2020.116078.

[174] Q. Wang, X. Ma, J. Xu, M. Li, and Y. Wang, "The three-regime-model for pseudo-boiling in supercritical pressure," *Int. J. Heat Mass Transf.*, vol. 181, pp. 121875, 2021. DOI:10.1016/j.ijheatmasstransfer.2021.121875.

[175] P.M. Tripathi, and S. Basu, "Insights into the dynamics of supercritical water flow using a two-phase approach," *Phys. Fluids*, vol. 33, no. 4, pp. 043304, 2021. DOI: 10.1063/5.0042935.

[176] J. Tamba, T. Ohara, and T. Aihara, "MD study on interfacelike phenomena in supercritical fluid," *Microscale Thermophys. Eng*., vol. 1, no. 1, pp. 19-30, 1997. DOI: 10.1080/108939597200395.

Table 1. List of recent experimental studies on supercritical CO_2 heated in circular tubes.

Literature	Flow direction	Tube diameter d_{in} (mm)	Inlet pressure P (MPa)	Mass flux G (kg/m^{2}s)	Heat flux q_w (kW/m^2)	Contents of study
Kim and Kim [33]	Vertical upward and downward	4.5	7.46-10.26	208-874	38-234	Heat transfer
Gupta et al. [34]	Vertical upward	8	7.4-8.8	900-3000	15-615	Heat transfer
Jiang et al. [35]	Vertical upward and downward	0.0992	7.7-9.7	1823-5043	85-748	Heat transfer
Tanimizu and Sadr [36]	Horizontal	8.7	7.5-9.0	185.04-285.97	16-64	Heat transfer
Zahlan et al. [38]	Vertical upward	8-22	7.44-8.67	197-2027	5.1-436	Heat transfer and pressure drop
Liu et al. [37]	Vertical upward and downward	6-10	7.4-10.6	298.8-1506.5	4.7-296.0	Heat transfer
Zhang et al. [39]	Vertical upward	16	7.5-10.5	50-500	5-100	Heat transfer
Zhu et al. [40]	Vertical upward	10	7.5-21.1	488-1600	74-413	Heat transfer
Guo et al. [41]	Horizontal	2	7.6-8.4	400-700	100-200	Heat transfer
Wang et al. [42]	Horizontal	0.5-1.0	7.6-9.0	58.1-4810	21.0-278.9	Heat transfer
Zhang et al. [43]	Vertical upward	8-12	7.5-23	400-1500	25-450	Heat transfer

Table 2. List of recent experimental studies on supercritical water heated in circular tubes.

Literature	Flow direction	Tube diameter d_{in} (mm)	Inlet pressure P (MPa)	Mass flux G (kg/m^{2}s)	Heat flux q_w (kW/m^2)	Contents of study
Zhu et al. [44]	Vertical upward	26	9-30	600-1200	200-600	Heat transfer
Mokry et al. [45]	Vertical upward	10	24	200-1500	70-1250	Heat transfer
Zhang et al. [46]	Vertical upward and downward	10	23-25	596-2021	772-1385	Heat transfer
Yu et al. [47]	Horizontal	26	23-25	300-700	200-400	Heat transfer
Yu et al. [48]	Horizontal	26-43	25	300-1000	400	Heat transfer
Shen et al. [49]	Vertical downward	17	11.5-28	450-1550	50-585	Heat transfer
Gu et al. [50]	Vertical upward	7.6-10	23-26	450-1500	190-1400	Heat transfer
Shen et al. [51]	Vertical upward	19	11-32	170-800	85-505	Heat transfer and pressure drop
Lei et al. [52]	Horizontal and vertical upward	26	23-28	200-1200	0-400	Heat transfer

Table 3. List of existing buoyancy parameters.

Literature	Parameter	Criteria	Flow direction	Fluid
Shiralkar and Griffith [76]	$Bu = \frac{Gr_{\mathrm{b}}}{Re_{\mathrm{b}}^{2}}$	Bu<0.01	Vertical upward and downward	CO_2
Jackson and Hall [77]	$Bu = \frac{Gr_{\mathrm{b}}}{Re_{\mathrm{b}}^{2.7}}$	Bu<10^{-4}	Horizontal	water
Deng et al. [78]	$Bu = \frac{\overline{Gr_{\mathrm{b}}}}{Re_{\mathrm{b}}^{2.7}}$	Bu<6×10^{-6}	Vertical upward and downward	kerosene
Jackson et al. [80]	$Bu = \frac{Gr^{*}}{Re_{\mathrm{b}}^{3.425}Pr^{0.8}}$	Bu<6×10^{-6}	Vertical upward and downward	water/CO_2
Liu et al. [37]	$Bu = \frac{Gr_b}{Pr_{\mathrm{w}}^{0.4}Re_{\mathrm{b}}^{2.625}}\left(\frac{\rho_{\mathrm{b}}}{\rho_{\mathrm{w}}}\right)^{0.5}(\frac{\mu_{\mathrm{w}}}{\mu_{\mathrm{b}}})$	Bu<1.3×10^{-5}	Vertical upward and downward	CO_2
Kim and Kim [81]	$Bu = \frac{Gr^{*}}{Pr^{0.8}Re_{\mathrm{b}}^{3.425}}\left(\frac{\rho_{\mathrm{b}}}{\rho_{\mathrm{w}}}\right)^{0.5}(\frac{\mu_{\mathrm{w}}}{\mu_{\mathrm{b}}})$	Not mentioned	Vertical upward	CO_2
Protopopov [83]	$Bu = (1-\frac{\rho_{\mathrm{w}}}{\rho_{\mathrm{b}}})\frac{Gr}{Re^{2}}$	Upward: Bu<0.01 downward: Always enhance	Vertical upward and downward	water/CO_2
Petukhov et al. [85]	$Bu = Gr^{*}Re_{\mathrm{b}}^{-2.75}Pr_{\mathrm{b}}^{-0.5}[1+2.4Re_{\mathrm{b}}^{-\frac{1}{8}}(Pr_{\mathrm{b}}^{\frac{2}{3}}-1)]^{-1}$	Bu<3×10^{-5}		
Liu et al. [82]	$Bu = \frac{\overline{Gr_{\mathrm{b}}}}{Re_{\mathrm{b}}^{2.7}}(\frac{\mu_{\mathrm{w}}}{\mu_{\mathrm{b}}})\left(\frac{\rho_{\mathrm{b}}}{\rho_{\mathrm{w}}}\right)^{0.5}$	Bu<2×10^{-5}	Vertical upward	CO_2
Hiroaki et al. [79]	$Bu = \frac{Re^{\frac{21}{8}}}{Gr}$ $Bu = \frac{Re^{\frac{21}{8}}Pr_{\mathrm{f}}^{0.4}}{Gr} \quad (for\ Pr_{\mathrm{f}} > 1)$	Bu>1.55×10^{3}	Vertical upward and downward	water

Seo et al. [84]	$\frac{1}{Fr}=\frac{1}{Re}\frac{\rho g d_{\mathrm{in}}}{\mu^2}(-\frac{\partial p}{\partial T}\Big\vert_p)\frac{q_{\mathrm{w}}}{(\frac{\lambda}{d_{\mathrm{in}}})Nu}$	$1/Fr<0.01$	Vertical upward	water

Table 4. List of existing flow acceleration parameters.

Literature	Parameter	Criteria	Flow direction	Fluid
McEligot et al. [87]	$Ac = \frac{4q_{\mathrm{w}}d_{\mathrm{in}}\beta_{\mathrm{b}}}{Re^2\mu_{\mathrm{b}}c_{\mathrm{p,b}}}$	$Ac<3\times10^{-6}$	Vertical upward and downward	CO_2
Kim and Kim [81]	$Ac = \frac{q^+}{Re_{\mathrm{b}}^{0.625}}(\frac{\mu_{\mathrm{w}}}{\mu_{\mathrm{b}}})\left(\frac{\rho_{\mathrm{b}}}{\rho_{\mathrm{w}}}\right)^{0.5}$	Not mentioned	Vertical upward	CO_2
Liu et al. [37]	$Ac = \frac{4q^+\alpha_{\mathrm{p}}T_{\mathrm{b}}}{d_{\mathrm{in}}}\frac{d_{\mathrm{in}}}{Re^{0.625}}(\frac{\mu_{\mathrm{w}}}{\mu_{\mathrm{b}}})\left(\frac{\rho_{\mathrm{b}}}{\rho_{\mathrm{w}}}\right)^{0.5}$	$Ac<3.3\times10^{-6}$	Vertical upward and downward	CO_2
Liu et al. [82]	$Ac = \frac{q_{\mathrm{w}}\beta}{Gc_{\mathrm{p,b}}Re_{\mathrm{b}}^{0.7}}(\frac{\mu_{\mathrm{w}}}{\mu_{\mathrm{b}}})\left(\frac{\rho_{\mathrm{b}}}{\rho_{\mathrm{w}}}\right)^{0.5}$	$Ac<4\times10^{-6}$	Vertical upward	CO_2
Hiroaki et al. [79]	$Ac = \frac{Re^{\frac{7}{8}}Pr_{\mathrm{f}}^{0.6}}{\frac{c_{\mathrm{p,f}}}{c_{\mathrm{p,b}}}\frac{\Delta T}{T_{\mathrm{b}}}}$	$Ac<246$	Vertical upward and downward	water
Jiang et al. [35]	$K_{\mathrm{v}} = K_{\mathrm{v,P}} + K_{\mathrm{v,T}} = -\frac{d_{\mathrm{in}}}{Re}\alpha_{\mathrm{T}}\frac{dp}{dx} + \frac{4q_{\mathrm{w}}d_{\mathrm{in}}\alpha_{\mathrm{p}}}{Re_{\mathrm{b}}^2\mu_{\mathrm{b}}c_{\mathrm{p}}}$	$K_{\mathrm{v}}<9.5\times10^{-7}$	Vertical upward and downward	CO_2
Gu et al. [86]	$Ac = \frac{q_{\mathrm{w}}d_{\mathrm{in}}\beta_{\mathrm{b}}}{\lambda_{\mathrm{b}}Re_{\mathrm{b}}^{1.63}Pr_{\mathrm{b}}}$	$Ac<10^{-6}$	Horizontal	methane

Table 5. Selected correlations for supercritical fluids heated in tubes.

Literature	Flow direction	Fluid	Tube diameter d_{in} (mm)	Inlet pressure P (MPa)	Correlation
Gupta et al. [34]	Vertical upward	CO_2	8	7.4-8.8	$Nu_b = 0.01 Re_b^{0.89} \overline{Pr_b}^{-0.14} (\frac{\rho_w}{\rho_b})^{0.93} (\frac{\lambda_w}{\lambda_b})^{0.22} (\frac{\mu_w}{\mu_b})^{-1.13}$ $Nu_f = 0.0043 Re_f^{0.94} (\frac{\rho_w}{\rho_b})^{0.57} (\frac{\lambda_w}{\lambda_b})^{-0.52}$ $Nu_w = 0.0038 Re_w^{0.96} \overline{Pr_w}^{-0.14} (\frac{\rho_w}{\rho_b})^{0.84} (\frac{\lambda_w}{\lambda_b})^{-0.75} (\frac{\mu_w}{\mu_b})^{-0.22}$
Kim and Kim [81]	Vertical upward	CO_2	4.5	7.46-10.26	$Nu_b = 0.226 Re_b^{1.174} Pr_{b,ave}^{1.057} (\frac{\rho_w}{\rho_b})^{0.42} (\frac{\overline{c_{p,b}}}{c_{p,b}})^{1.023} Ac^{0.489} Bu^{0.0021}$ $Ac = \frac{q_w \beta_b}{G c_{p,b} Re_b^{0.625}} (\frac{\mu_w}{\mu_b}) \left(\frac{\rho_b}{\rho_w}\right)^{0.5}$ $Bu = \frac{Gr_q}{Re_b^{3.425} Pr_w^{0.8}} \left(\frac{\rho_b}{\rho_w}\right)^{0.5} (\frac{\mu_w}{\mu_b})$ $Gr_q = \frac{g \beta_b d_i^4 q_w}{\nu_b^2 \lambda_b}$, $\overline{c_{p,b}} = \frac{i_w - i_b}{T_w - T_b}$
Zhu et al. [98]	Vertical upward	CO_2	10	7.52-20.8	$Nu = 0.0012 Re_b^{0.9484} Pr_{b,ave}^{0.718} K^{-0.0313}$ $K = (\frac{q}{G i_w})^2 \frac{\rho_b}{\rho_w}$
Bae et al. [94]	Vertical upward	CO_2	4.4, 9	7.75-8.85	$Nu = 0.021 Re_b^{0.82} Pr_b^{0.5} \left(\frac{\rho_w}{\rho_b}\right)^{0.3} \left(\frac{\overline{c_{p,b}}}{c_{p,b}}\right)^n f(Bu)$ $Bu = \frac{\overline{Gr_b}}{Re_b^{2.7} \overline{Pr_b}^{0.5}}$

Liu et al. [37]	Vertical upward and downward	CO_2	6, 10	7.4-10.6	$f(Bu) = \begin{cases} (1+10^8 Bu)^{-0.032} & when\ \ 5\times10^{-8} < Bu < 7\times10^{-7} \\ 0.0185 Bu^{-0.43465} & when\ \ 7\times10^{-7} < Bu < 1\times10^{-6} \\ 0.75 & when\ \ 1\times10^{-6} < Bu < 1\times10^{-5} \\ 0.0119 Bu^{-0.36} & when\ \ 1\times10^{-5} < Bu < 3\times10^{-5} \\ 32.4 Bu^{0.4} & when\ \ 3\times10^{-5} < Bu < 1\times10^{-4} \end{cases}$ $Nu_{\mathrm{b}} = 0.00075 Re_{\mathrm{b}}^{0.93} \overline{Pr_{\mathrm{b}}}^{0.68} \left(\frac{\rho_{\mathrm{w}}}{\rho_{\mathrm{b}}}\right)^{0.42} \times \exp\left(Bu^{-0.023}\right) \times \exp\left(Ac^{0.079}\right)[1 + 2.63/(l/d_{\mathrm{i}})]$ $Bu = \frac{Gr_{\mathrm{b}}}{Re_{\mathrm{b}}^{2.625} Pr_{\mathrm{w}}^{0.4}} \left(\frac{\rho_{\mathrm{b}}}{\rho_{\mathrm{w}}}\right)^{0.5} \left(\frac{\mu_{\mathrm{w}}}{\mu_{\mathrm{b}}}\right)$ $Ac = \frac{4q\alpha_{\mathrm{p}}}{Gc_{\mathrm{p,b}} Re_{\mathrm{b}}^{0.625}} \left(\frac{\mu_{\mathrm{w}}}{\mu_{\mathrm{b}}}\right) \left(\frac{\rho_{\mathrm{b}}}{\rho_{\mathrm{w}}}\right)^{0.5}$
Jackson [95]	Vertical upward and downward	CO_2	Obtained by reviewing existing literature and data		$Nu = 0.0183 Re_{\mathrm{b}}^{0.82} Pr_{\mathrm{b}}^{0.5} \left(\frac{\rho_{\mathrm{w}}}{\rho_{\mathrm{b}}}\right)^{0.3} \left(\frac{c_{\mathrm{p,ave}}}{c_{\mathrm{p,b}}}\right)^{n}$ $n = \begin{cases} 0.4; \ \ T_{\mathrm{b}} < T_{\mathrm{w}} < T_{\mathrm{pc}} \ \ or \ \ T_{\mathrm{pc}} < T_{\mathrm{b}} < T_{\mathrm{w}} \\ 0.4 + 0.2\left(\frac{T_{\mathrm{w}}}{T_{\mathrm{pc}}} - 1\right); \ \ T_{\mathrm{b}} < T_{\mathrm{pc}} < T_{\mathrm{w}} \\ 0.4 + 0.2\left(\frac{T_{\mathrm{w}}}{T_{\mathrm{pc}}} - 1\right)\left[1 - 5\left(\frac{T_{\mathrm{b}}}{T_{\mathrm{pc}}} - 1\right)\right]; \ \ T_{\mathrm{pc}} < T_{\mathrm{b}} < 1.2T_{\mathrm{pc}} \end{cases}$
Swenson et al. [61]	Vertical upward	water	9.43	22.8-41.4	$Nu_{\mathrm{w}} = 0.00459 Re_{\mathrm{w}}^{0.923} Pr_{\mathrm{w,ave}}^{0.613} \left(\frac{\rho_{\mathrm{w}}}{\rho_{\mathrm{b}}}\right)^{0.231}$ $Pr_{\mathrm{w,ave}} = \frac{\mu_{\mathrm{w}}}{\lambda_{\mathrm{w}}} \frac{i_{\mathrm{w}} - i_{\mathrm{b}}}{T_{\mathrm{w}} - T_{\mathrm{b}}}$
Bishop et al. [96]	Vertical upward	water	2.50-5.08	22.6-27.6	$Nu = 0.0069 Re_{\mathrm{b}}^{0.9} Pr_{\mathrm{b,ave}}^{0.66} \left(\frac{\rho_{\mathrm{w}}}{\rho_{\mathrm{b}}}\right)^{0.43} \left(1 + \frac{2.4}{L/d_{\mathrm{in}}}\right)$
Yu et al. [97]	Vertical upward and downward	water	1.5-38.1	22.6-41	$Nu = 0.0138 Re_{\mathrm{b}}^{0.9078} Pr_{\mathrm{b,ave}}^{0.6171} \left(\frac{\rho_{\mathrm{w}}}{\rho_{\mathrm{b}}}\right)^{0.4356} Gr^{-0.012} (q^{+})^{0.0605}$

					$q^+ = \frac{q_w \beta_b}{G c_p}$
Mokry et al. [45]	Vertical upward	water	10	24	$Nu = 0.0138 Re_b^{0.9078} Pr_{b,ave}^{0.6171} \left(\frac{\rho_w}{\rho_b}\right)^{0.4356} Gr^{-0.012} (q^+)^{0.0605}$
Shen et al. [51]	Vertical downward	water	17	22.5-28	$Nu_w = 0.00677 Re_w^{0.883} \left(\left(\frac{h_w - h_f}{T_w - T_f}\right)\frac{\mu_w}{\lambda_w}\right)^{0.602} \left(\frac{\nu_f}{\nu_w}\right)^{0.346}$ when $h_b < h_{pc}$ $Nu_w = 0.127 Re_w^{0.682} ((\frac{h_w - h_f}{T_w - T_f})\frac{\mu_w}{\lambda_w})^{1.06} (\frac{\nu_f}{\nu_w})^{0.976}$, when $h_b \geq h_{pc}$

Table 6. List of recent experimental studies on supercritical CO_2 cooled in tubes.

Literature	Channel configuration and material	Flow direction	Tube diameter d_{in} (mm)	Inlet temperature T_{in} (°C)	Inlet pressure P (MPa)	Mass flux G (kg/m^{2}s)	Contents of study
Dang and Hihara [126]	Single circular, copper	Horizontal	1-6	30-70	8-10	200-1200	Heat transfer and pressure drop
Son and Park [127]	Single circular, stainless steel	Horizontal	7.75	90-100	7.5-10	200-400	Heat transfer and pressure drop
Oh et al. [128]	Helically coiled tube, copper	Horizontal	4.55-6.35	80-90	7.5-10	200-800	Heat transfer and pressure drop
Bruch et al. [129]	U-shape pipe, copper	Vertical	6	40-70	7.4-12	50-590	Heat transfer
Liu et al. [130]	Single circular, copper	Horizontal	4-10.7	32-67	7.5-8.5	74.14-795.77	Heat transfer and pressure drop
Ma et al.[135]	Single circular, stainless-steel	Vertical	16	50-80	8-10	491-823	Heat transfer
Wang et al. [131]	Helically coiled tube, copper	Horizontal and vertical	4	41.85-56.85	8.0042-9.0072	159.0-318.2	Heat transfer
Zhang et al. [132]	Single circular, stainless steel	Horizontal	4-10	77-97	8-9	160-320	Heat transfer
Liu et al. [133]	Helically coiled tube, copper	Horizontal	4-6	20-55	7.5-9	35.37-318.31	Heat transfer
Lei et al. [134]	Single circular, stainless steel	Horizontal and vertical	1	34.41-42.09	7.5-8.2	467.92-907.89	Heat transfer

Table 7. Selected correlations for supercritical CO_2 cooled in tubes.

Literature	Flow direction	Fluid	Tube diameter d_{in} (mm)	Inlet pressure P (MPa)	Correlation
Liao et al. [136]	horizontal	CO_2	0.5-2.16	7.4-12	$Nu_w = 0.128 Re_w^{0.8} Pr_w^{0.3} \left(\frac{\rho_b}{\rho_w}\right)^{0.437} \left(\frac{\bar{c_p}}{c_{pw}}\right)^{0.411} \left(\frac{Gr}{Re_b^2}\right)^{0.205}$
Yoon et al. [137]	horizontal	CO_2	7.73	7.5-8.8	$Nu_w = 1.38 Nu'_w \left(\frac{\rho_w}{\rho_b}\right)^{0.57} \left(\frac{\bar{c_p}}{c_{pw}}\right)^{0.86}$ $Nu_b = a Re_b^b Pr_b^c \left(\frac{\rho_{pc}}{\rho_b}\right)^n$ $a = 0.14, b = 0.69, c = 0.66, n = 0$ for $T_b > T_{pc}$ $a = 0.013, b = 1.0, c = -0.05, n = 1.6$ for $T_b \le T_{pc}$
Dang et al. [126]	horizontal	CO_2	1-6	8-10	$h = Nu\, \lambda_f / d$ $Nu = \frac{(f_f/8)(Re_b - 1000)Pr}{1.07 + 12.7\sqrt{\frac{f_f}{8}}(Pr^{\frac{2}{3}} - 1)}$ $Pr = \begin{cases} c_{p_b}\mu_b/\lambda_b, & for\ c_{p_b} \ge \bar{c_p} \\ \bar{c_p}\mu_b/\lambda_b, & for\ c_{p_b} < \bar{c_p} \text{ and } \mu_b/\lambda_b \ge \mu_f/\lambda_f \\ \bar{c_p}\mu_f/\lambda_f, & for\ c_{p_b} < \bar{c_p} \text{ and } \mu_b/\lambda_b < \mu_f/\lambda_f \end{cases}$ $\bar{c_p} = b(h_b - h_w)/(T_b - T_w), Re_b = Gd/\mu_b$ $f_f = [1.82 log10(Re_f) - 1.64]^{-2}, Re_f = Gd/\mu_f$
Son et al. [127]	horizontal	CO_2	7.75	7.5-10	$Nu_b = Re_b^{0.55} Pr_b^{0.23} \left(\frac{c_{p,b}}{c_{p,w}}\right)^{0.411} \left(\frac{Gr}{Re_b^2}\right)^{0.15}$ for $T_b/T_{pc} > 1$ $Nu_b = Re_b^{0.35} Pr_b^{1.9} \left(\frac{\rho_b}{\rho_w}\right)^{-1.6} \left(\frac{c_{p,b}}{c_{p,w}}\right)^{-3.4}$ for $T_b/T_{pc} \le 1$
Oh et al. [138]	horizontal	CO_2	4.55-7.75	7.5-10	$Nu_b = a' Re_b^{b'} Pr_b^{c'} \left(\frac{\rho_b}{\rho_w}\right)^{d'} \left(\frac{c_{p,b}}{c_{p,w}}\right)^{e'}$

					$a' = 0.023, b' = 0.7, c' = 2.5, d' = 0, e' = -3.5$ $for\ T_b/T_{pc} > 1$ $a' = 0.023, b' = 0.6, c' = 3.2, d' = 3.7, e' = -4.6$ $for\ T_b/T_{pc} \leq 1$
Liu et al. [130]	horizontal	CO_2	4-10.7	7.5-8.5	$Nu_w = 0.01 Re_w^{0.9} Pr_w^{0.5} \left(\frac{\rho_w}{\rho_b}\right)^{0.906} \left(\frac{c_{p,w}}{c_{p,b}}\right)^{-0.585}$
Ma et al. [135]	downward	CO_2	12	8-10	$\frac{Nu_b}{Nu_{FC}} = 2.61 - 86.965 \left(\frac{Gr}{Re_b^{2.7}}\right)^{0.458}$ $where\ 8 \times 10^4 < Re < 4.9 \times 10^5$ and $11 < Pr < 130$ $Nu_{FC} = 0.0183 Re_b^{0.82} Pr_b^{0.5} \left(\frac{\rho_b}{\rho_w}\right)^{-0.3}$
Zhang et al. [132]	horizontal	CO_2	4-10	8-9	$Nu_f = 0.138 Re_b^{0.68} Pr_f^{0.07} \left(\frac{\rho_f}{\rho_w}\right)^{-0.74} \left(\frac{\overline{c_{p,b}}}{c_{p,b}}\right)^{-0.31}$ $(\frac{Gr_g}{Re^2})^{0.08}[1 + (\frac{d}{L})^{2/3}]$
Pitla et al. [139]	horizontal	CO_2	4.72	8-13.4	$Nu = (\frac{Nu_b + Nu_w}{2}) \frac{\lambda_w}{\lambda_b}$ where Nu_b and Nu_w are calculated using the following correlation formula $Nu = \frac{(f/8)(Re - 1000)Pr}{1.07 + 12.7\sqrt{f/8}(Pr^{2/3} - 1)}$ $f = (0.79 \ln(Re) - 1.64)^{-2}$ $h = \frac{Nu}{d} \lambda_b$

List of figure captions

Figure 1. (a) Schematic of the recompression supercritical CO_2 Brayton cycle. Replotted from Ref. [7]. (b) Schematic of the transcritical CO_2 refrigeration cycle with internal heat exchanger. Reproduced with permission from Ref. [12]. Copyright 2019, Elsevier.

Figure 2. Variation of the thermophysical properties of supercritical fluids: (a) supercritical water at 24 MPa; (b) supercritical CO_2 at 9 MPa.

Figure 3. Wall temperature and HTC profiles for two regimes of supercritical heat transfer: (a) normal heat transfer with smooth temperature profile, and (b) heat transfer deterioration with a temperature peak. Data obtained from Ref. [40] for supercritical CO_2 flowing upward in a vertical tube with inner diameter of 10 mm. Experimental conditions: (a) pressure 8.221 MPa, heat flux 244.33 kW/m^2, mass flux 744.5 kg/m^{2}s; (b) pressure 20.822 MPa, heat flux 355.45 kW/m^2, mass flux 1001.5 kg/m^{2}s.

Figure 4. Variations of wall temperature and heat transfer coefficient with the bulk fluid enthalpy for supercritical water heated in a horizontal tube with inner diameter of 26 mm. The experimental pressure, heat flux, and mass flux are 25 MPa, 300 kW/m^2, and 600 kg/m^{2}s, respectively. Data obtained from Ref. [47].

Figure 5. Heat transfer coefficient variation with bulk fluid temperature for cooling heat transfer of CO_2 under various pressures. Replotted from Ref. [130].

Figure 6. Snapshots of MD simulation cell for supercritical argon in liquid-like, two-phase-like, and gas-like regimes at pressures far above the critical pressure. P_r and T_r represent reduced pressure (P/P_c, P_c is the critical pressure) and reduced temperature (T/T_c, T_c is the critical temperature), respectively. Reproduced with permission from Ref. [169]. Copyright 2021, American Physical Society.

Figure 7. (a) The wall temperature rise as a function of *SBO* for SCO_2 heated in vertical upward tubes., showing a critical SBO=5.126×10^{-4} as the transition boundary between NHT and HTD. Reproduced with permission from Ref. [40]. Copyright 2018, Elsevier. (b) Friction factor *f* as a function of *Re*, showing a larger *f* in multi-peak cases due to the multiple orifice contraction events. Reproduced with permission from Ref. [43]. Copyright 2021, Elsevier.

Figure 8. Nu/Nu_{DB} versus pseudo-vapor mass quality x for (a) supercritical water and (b) supercritical CO_2, where Nu is the experimentally measured Nusselt number and Nu_{DB} is the calculated Nusselt number using the Dittus-Boelter correlation. The ratio approaches 1 in the liquid-like (LL) and vapor-like (VL) (same as gas-like, GL) regimes, while significantly deviates from 1 in the two-phase-like (TPL) regime with $0<x<1$. Reproduced with permission from Ref. [174]. Copyright 2021, Elsevier.

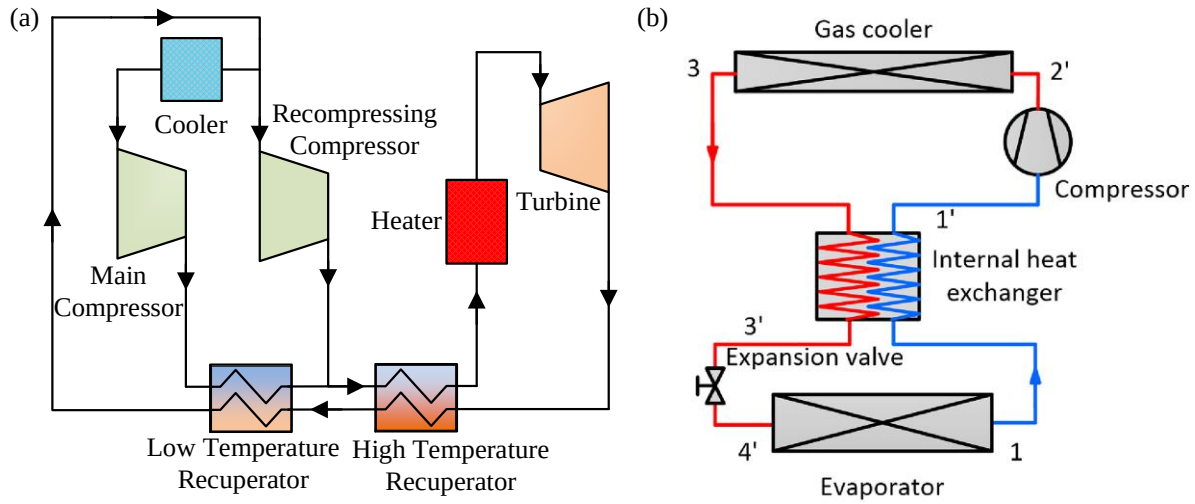

Figure 1. (a) Schematic of the recompression supercritical CO_2 Brayton cycle. Replotted from Ref. [7]. (b) Schematic of the transcritical CO_2 refrigeration cycle with internal heat exchanger. Reproduced with permission from Ref. [12]. Copyright 2019, Elsevier.

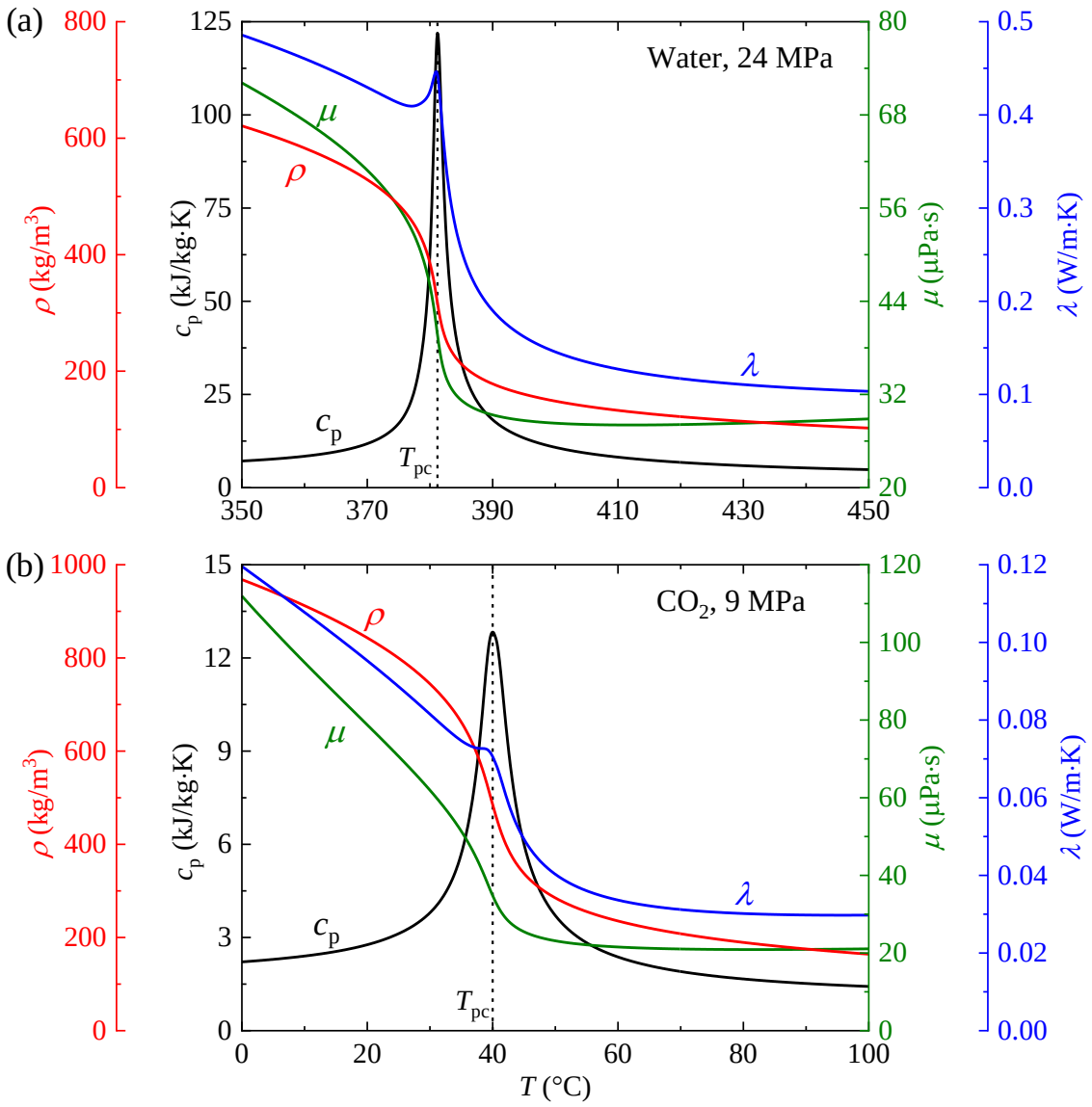

Figure 2. Variation of the thermophysical properties of supercritical fluids: (a) supercritical water at 24 MPa; (b) supercritical CO_2 at 9 MPa.

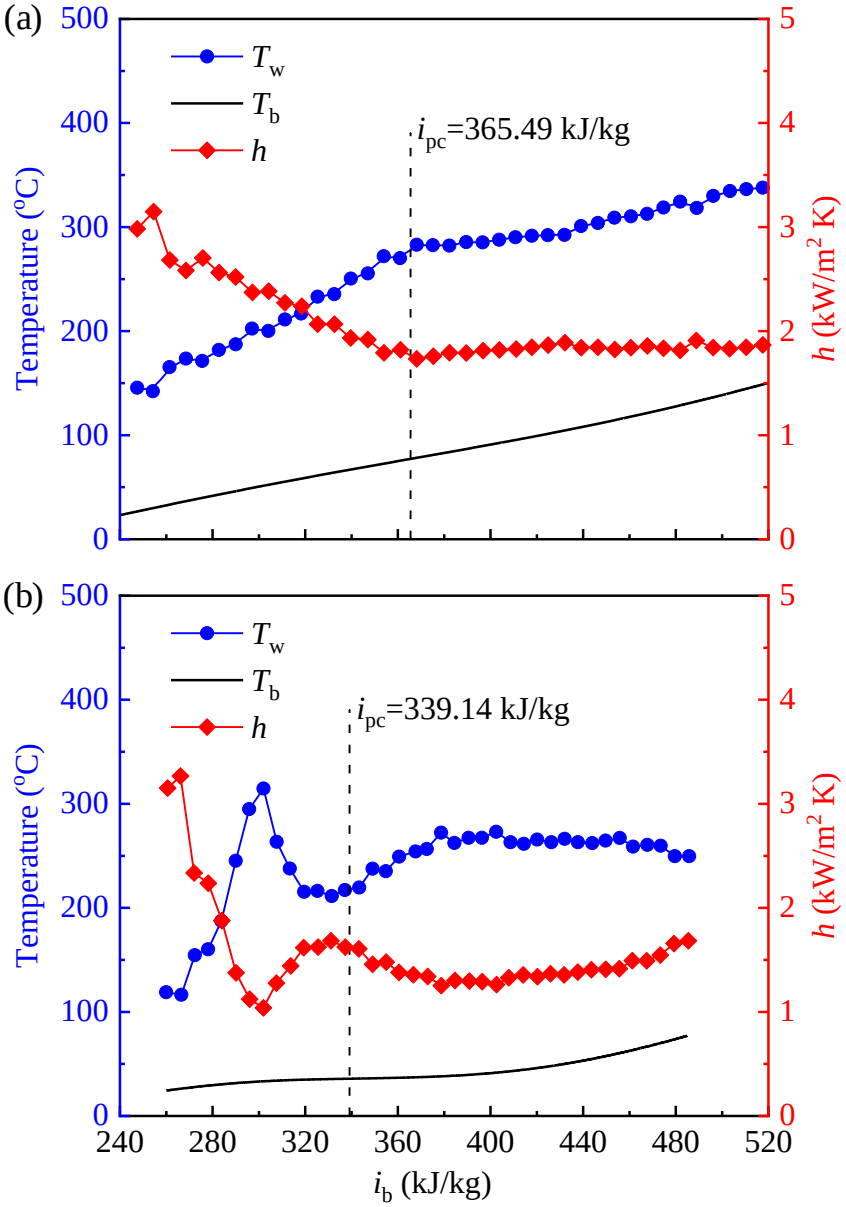

Figure 3. Wall temperature and HTC profiles for two regimes of supercritical heat transfer: (a) normal heat transfer with smooth temperature profile, and (b) heat transfer deterioration with a temperature peak. Data obtained from Ref. [40] for supercritical CO_2 flowing upward in a vertical tube with inner diameter of 10 mm. Experimental conditions: (a) pressure 8.221 MPa, heat flux 244.33 kW/m^2, mass flux 744.5 kg/m^{2}s; (b) pressure 20.822 MPa, heat flux 355.45 kW/m^2, mass flux 1001.5 kg/m^{2}s.

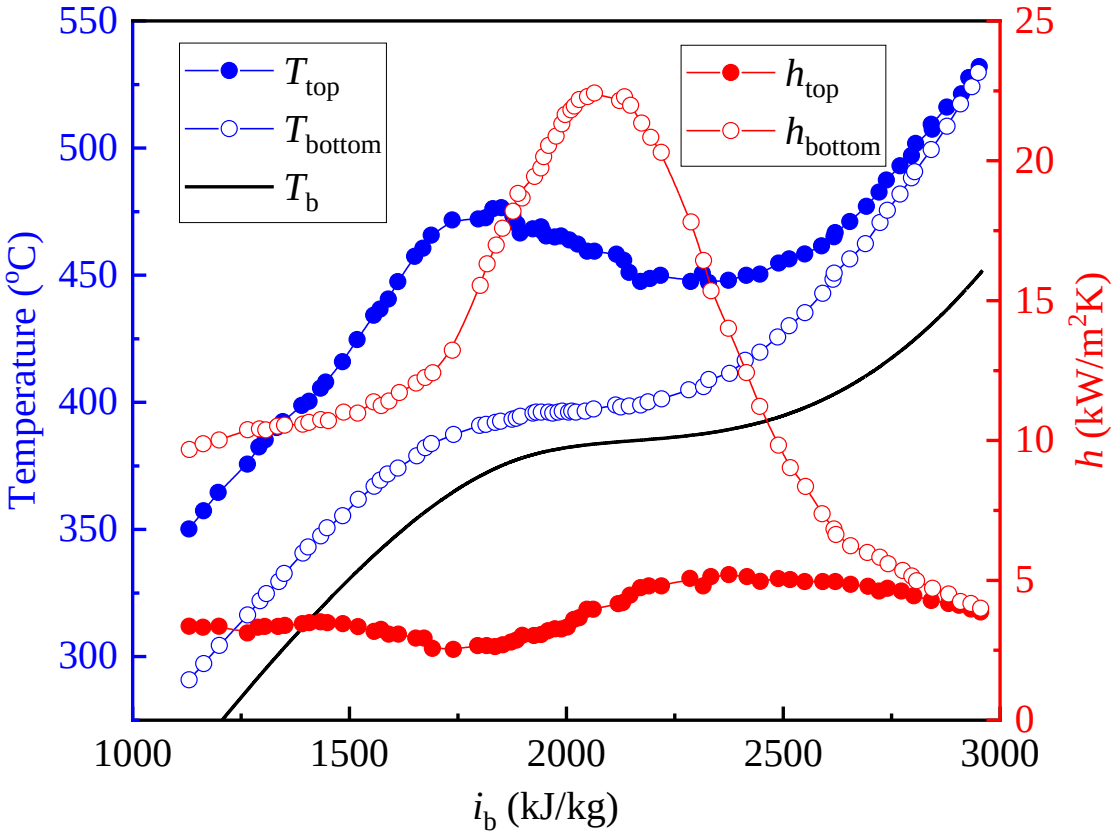

Figure 4. Variations of wall temperature and heat transfer coefficient with the bulk fluid enthalpy for supercritical water heated in a horizontal tube with inner diameter of 26 mm. The experimental pressure, heat flux, and mass flux are 25 MPa, 300 kW/m^2, and 600 kg/m^{2}s, respectively. Data obtained from Ref. [47].

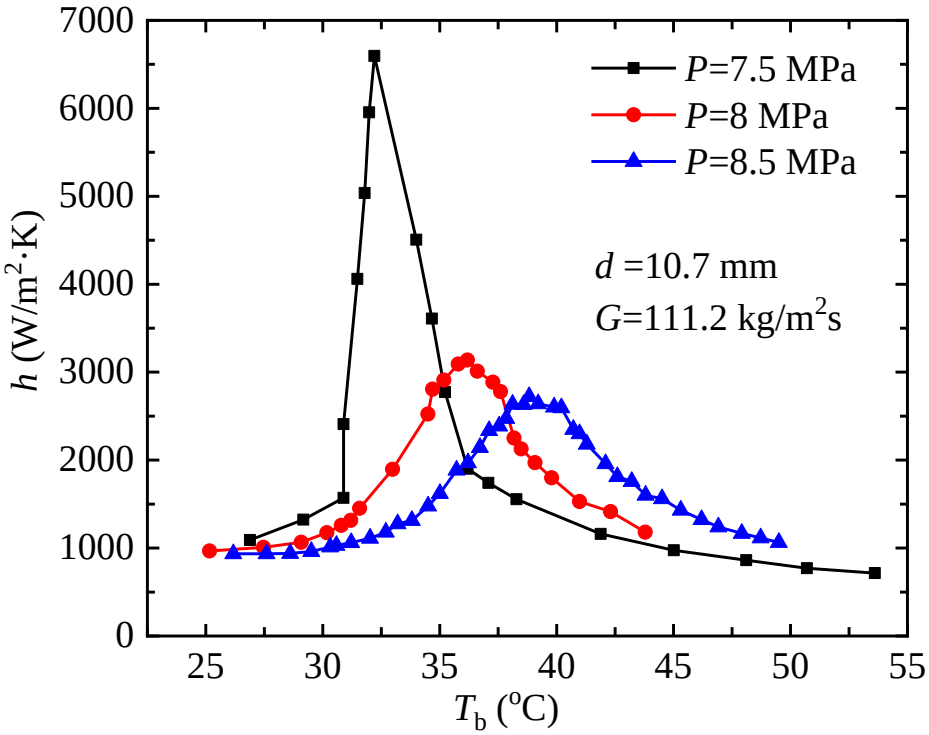

Figure 5. Heat transfer coefficient variation with bulk fluid temperature for cooling heat transfer of CO_2 under various pressures. Replotted from Ref. [130].

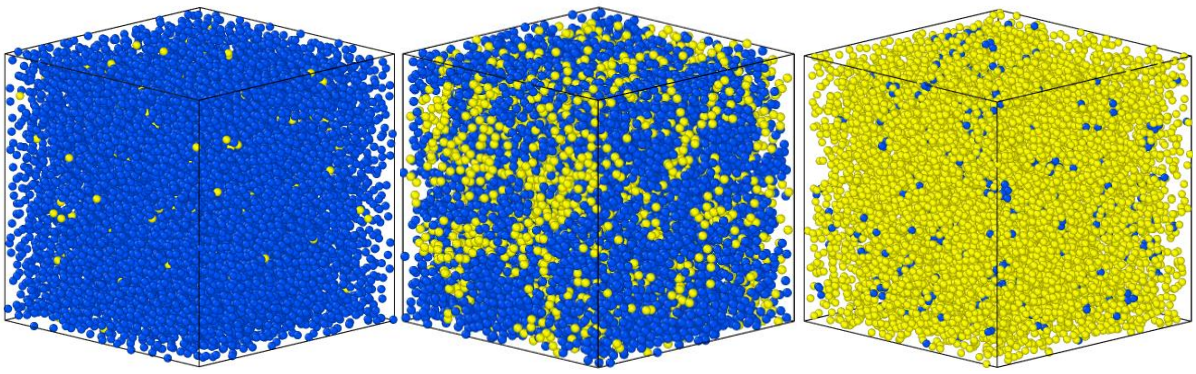

Figure 6. Snapshots of MD simulation cell for supercritical argon in liquid-like, two-phase-like, and gas-like regimes at pressures far above the critical pressure. P_r and T_r represent reduced pressure (P/P_c, P_c is the critical pressure) and reduced temperature (T/T_c, T_c is the critical temperature), respectively. Reproduced with permission from Ref. [169]. Copyright 2021, American Physical Society.

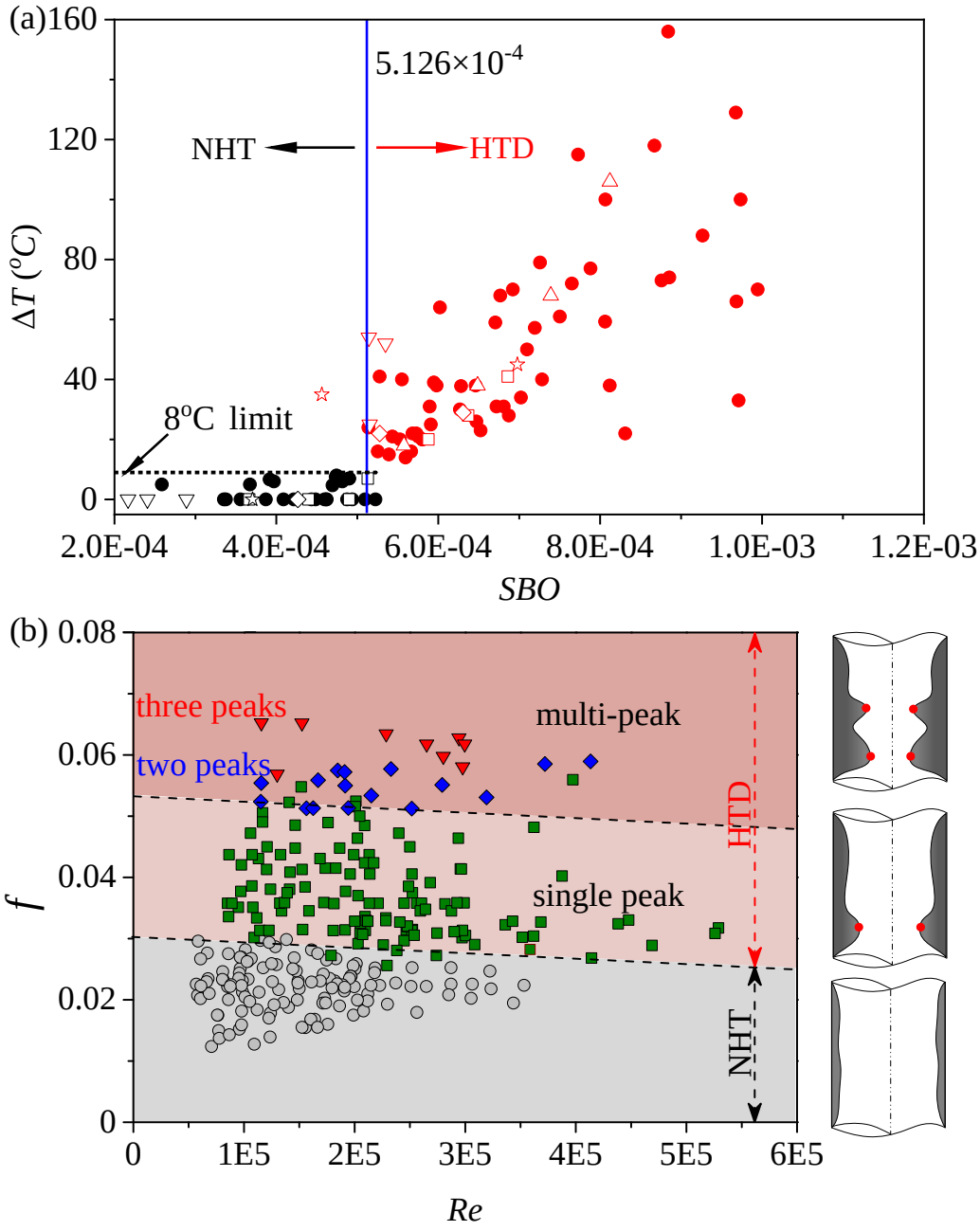

Figure 7. (a) The wall temperature rise as a function of *SBO* for SCO_2 heated in vertical upward tubes., showing a critical $SBO=5.126\times10^{-4}$ as the transition boundary between NHT and HTD. Reproduced with permission from Ref. [40]. Copyright 2018, Elsevier. (b) Friction factor *f* as a function of *Re*, showing a larger *f* in multi-peak cases due to the multiple orifice contraction events. Reproduced with permission from Ref. [43]. Copyright 2021, Elsevier.

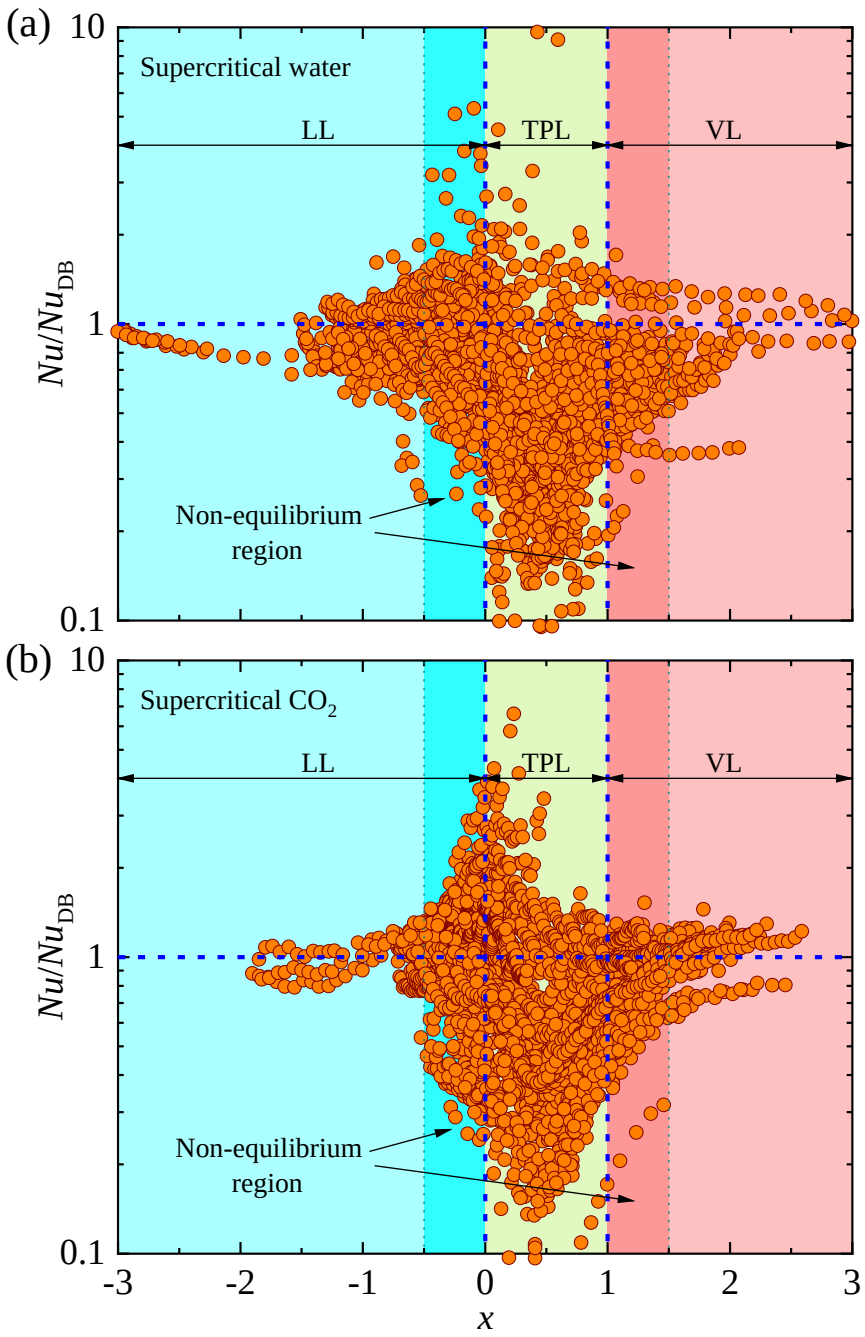

Figure 8. Nu/Nu_{DB} versus pseudo-vapor mass quality x for (a) supercritical water and (b) supercritical CO_2, where Nu is the experimentally measured Nusselt number and Nu_{DB} is the calculated Nusselt number using the Dittus-Boelter correlation. The ratio approaches 1 in the liquid-like (LL) and vapor-like (VL) (same as gas-like, GL) regimes, while significantly deviates from 1 in the two-phase-like (TPL) regime with $0<x<1$. Reproduced with permission from Ref. [174]. Copyright 2021, Elsevier.

Notes on contributors

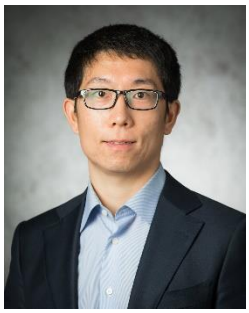

Qingyang Wang is an associate professor in the School of Energy Power and Mechanical Engineering at North China Electric Power University. He obtained his B.Eng. in energy power system and automation from Tsinghua University in 2015, and Ph.D. in mechanical engineering from University of California San Diego in 2020. His research interests include micro/nanoscale heat transfer, phase change heat transfer and multiphase flow, and supercritical energy transport and conversion.

Jinliang Xu is a professor at School of Energy Power and Mechanical Engineering, North China Electric Power University. He is currently the Director of Beijing Key Laboratory of Multiphase Flow and Heat Transfer for Low Grade Energy Utilization. His research interest includes multiphase flow and heat transfer in micro/nano systems, advanced power generation system, low grade energy and renewable energy utilization. He has published over 200 international journal papers as corresponding author and co-authored two books. He has been the chair or co-chair for multiple international conferences, the editor or associate editor of multiple journals including Energies, Thermal Science and Engineering Progress, Frontiers in Heat pipe, and Alternative Energy, and the guest editor for the special issue of Applied Thermal Engineering and Energy. He has presented over 40 keynote speeches in international conferences and has been the reviewer for more than 30 journals. He received the Natural Science Award of the Ministry of Education, China (first grade) in 2012. He has been the “973”

project chief scientist, Ministry of Science in 2011 and was awarded as “Yangtze River Scholar” Professor by the National Ministry of education, China in 2013.

Chengrui Zhang is a master student in North China Electric Power University, majoring in power engineering and engineering thermophysics. He received a bachelor’s degree in engineering from Anhui University of Science and Technology. He is currently working in the Beijing Key Laboratory of Multiphase Flow and Heat Transfer for Low Grade Energy Utilization. He is devoted to the experimental investigation of supercritical carbon dioxide heat transfer.

Bingtao Hao is a master student in the School of Energy, Power and Mechanical Engineering at North China Electric Power University. He received his bachelor’s degree from Harbin University of Commerce. He is working in the Beijing Key Laboratory of Multiphase Flow and Heat Transfer for Low Grade Energy Utilization on flow and heat transfer of supercritical carbon dioxide.

Lixin Cheng has worked at Sheffield Hallam University since 2016. He obtained his Ph.D. in Thermal Energy Engineering at the State Key Laboratory of Multiphase Flow at Xi’an Jiaotong University, China in 1998. He has received several prestigious awards such as Alexander von Humboldt Fellowship in Germany in 2006, an ERCOFTAC Visitor Grant in Switzerland in

2010 and a Distinguished Visiting Professorship of the City of Beijing, China in 2015. His research interests include multiphase flow and heat transfer and thermal energy engineering. He has published more than 100 papers in journals and conferences, 9 book chapters and edited 10 books. He has delivered more than 60 keynote and invited lectures worldwide. He has been the chair of the *World Congress on Momentum, Heat and Mass Transfer* (*MHMT*) since 2017. He is one of the founders and co-chair of the *International Symposium of Thermal-Fluid Dynamics* (*ISTFD*) series since 2019. He is associate editor of *Heat Transfer Engineering* and *Journal of Fluid Flow, Heat and Mass Transfer*, and international advisor of *Thermal Power Generation* (a Chinese journal).